Annals of Botany **128**: 261–280, 2021
doi: 10.1093/aob/mcab044, available online at www.academic.oup.com/aob

ANNALS OF BOTANY
Founded 1887

Divergence in floral scent and morphology, but not thermogenic traits, associated with pollinator shift in two brood-site-mimicking *Typhonium* (Araceae) species

Thomas D. J. Sayers[1,*], Kim L. Johnson[2], Martin J. Steinbauer[3], Kevin Farnier[3,4] and Rebecca E. Miller[1,5]

[1]School of Ecosystem and Forest Sciences, The University of Melbourne, 500 Yarra Blvd, Richmond, VIC 3121, Australia, [2]Department of Animal, Plant and Soil Sciences, La Trobe University, Bundoora, VIC 3086, Australia, [3]Department of Ecology, Environment and Evolution, La Trobe University, Melbourne, VIC 3086, Australia, [4]Department of Jobs, Precincts and Regions, Agriculture Victoria, Melbourne, VIC 3083, Australia and [5]Royal Botanic Gardens Victoria, South Yarra, VIC, 3141, Australia
**For correspondence. E-mail tdjsayers@gmail.com*

Received: 8 December 2020 Returned for revision: 9 February 2021 Editorial decision: 18 March 2021 Accepted: 20 March 2021
Electronically published: 24 March 2021

• **Background** Flowers which imitate insect oviposition sites probably represent the most widespread form of floral mimicry, exhibit the most diverse floral signals and are visited by two of the most speciose and advanced taxa of insect – beetles and flies. Detailed comparative studies on brood-site mimics pollinated exclusively by each of these insect orders are lacking, limiting our understanding of floral trait adaptation to different pollinator groups in these deceptive systems.
• **Methods** Two closely related and apparent brood-site mimics, *Typhonium angustilobum* and *T. wilbertii* (Araceae) observed to trap these distinct beetle and fly pollinator groups were used to investigate potential divergence in floral signals and traits most likely to occur under pollinator-mediated selection. Trapped pollinators were identified and their relative abundances enumerated, and thermogenic, visual and chemical signals and morphological traits were examined using thermocouples and quantitative reverse transcription–PCR, reflectance, gas chromatography–mass spectrometry, floral measurements and microscopy.
• **Key Results** *Typhonium angustilobum* and *T. wilbertii* were functionally specialized to trap saprophagous Coleoptera and Diptera, respectively. Both species shared similar colour and thermogenic traits, and contained two highly homologous *AOX* genes (*AOX1a* and *AOX1b*) most expressed in the thermogenic tissue and stage (unlike *pUCP*). Scent during the pistillate stage differed markedly – *T. angustilobum* emitted a complex blend of sesquiterpenes, and *T. wilbertii*, a dung mimic, emitted high relative amounts of skatole, *p*-cresol and irregular terpenes. The species differed significantly in floral morphology related to trapping mechanisms.
• **Conclusions** Functional specialization and pollinator divergence were not associated with differences in anthesis rhythm and floral thermogenic or visual signals between species, but with significant differences in floral scent and morphological features, suggesting that these floral traits are critical for the attraction and filtering of beetle or fly pollinators in these two brood-site mimics.

Key words: Alternative oxidase, Araceae, brood-site mimicry, cantharophily, Coleoptera, Diptera, floral volatile organic compounds, floral trap, sapromyophily, thermogenesis, *Typhonium angustilobum*, *Typhonium wilbertii.*

INTRODUCTION

Plant–pollinator interactions typically involve a process of co-evolution involving the reciprocal adaptation of pollinators to the most rewarding floral traits (Thompson, 1994). Of the approx. 300 000 animal-pollinated angiosperms, however, at least 7500 plant species have evolved the ability to advertise the presence of a reward without providing it (Dafni, 1984; Renner, 2006; Ollerton *et al.*, 2011; Schaefer and Ruxton, 2011; Johnson and Schiestl, 2016). In the absence of a reward, deceptive signals and/or cues (i.e. olfactory, visual, tactile, gustatory and thermal) play a more prominent role in pollinator attraction. Deceptive flowers are hypothesized to emit signals evolved to exploit the pre-existing receiver bias in the response pathways of the pollinator's sensory systems acquired outside the context of plant–pollinator interactions or flower visitation (Schiestl and Dötterl, 2012; Schiestl and Johnson, 2013). Several types of floral mimics have been identified, including species which mimic food sources, sexual partners and oviposition sites (Dafni, 1984). Oviposition or brood-site mimics, which model diverse decomposing substrates (e.g. dung, carrion, fermenting fruit and fungi), are considered the most widespread form of floral mimicry, occurring in at least 23 plant families (Urru *et al.*, 2011; Jürgens *et al.*, 2013; Johnson and Schiestl, 2016). They are also the most diverse in terms of floral signalling (Johnson and Schiestl, 2016), making them good systems in which to investigate pollinator and floral trait diversification.

To attract pollinators, brood-site mimics have developed complex and varied floral volatile organic compounds (VOCs) and dull floral pigmentations and patterns (e.g. brown, purple

and spotted) which may both resemble a model substrate and be vital for multisensory pollinator attraction (Kite *et al.*, 1998; Jürgens *et al.*, 2013; Chen *et al.*, 2015; Johnson *et al.*, 2020). Brood-site mimics often also exhibit inflorescences or flowers with a floral chamber which trap and force insects close to the floral reproductive organs during anthesis (Bröderbauer *et al.*, 2012; Johnson and Schiestl, 2016). Another common trait of brood-site mimics and most prevalent in early diverging seed plants (e.g. Cycadales, magnoliids, monocots and some eudicots) is floral thermogenesis, the timing, intensity, duration and location of which can vary markedly between thermogenic plant species, including congeneric species (Meeuse and Raskin, 1988; Seymour and Schultze-Motel, 1997; Seymour *et al.*, 2009*a*; Sayers *et al.*, 2020). The prevalence of thermogenesis in early seed plants raises questions about the role of thermogenesis in the origin of pollination, yet research tends to focus on the evolution and role of visual and olfactory signals (van der Kooi and Ollerton, 2020). The main hypothesized functions of floral heat are that it is an energy reward (Seymour and Matthews, 2006), a deceptive signal for pollinators to associate with a rewarding substrate (e.g. carrion and dung) (Angioy *et al.*, 2004; Schiestl, 2017), that it enhances scent volatilization (Marotz-Clausen *et al.*, 2018) and that it plays a role in floral development (Li and Huang, 2009). In brood-site mimetic systems, it is most likely that heat production acts as a direct signal for pollinators in conjunction with scent volatilization and other signals, as shown in the araceous carrion mimic *Helicodiceros muscivorus* (Angioy *et al.*, 2004; Schiestl, 2017). The function(s) of thermogenesis in other brood-site mimetic systems and its significance to different pollinator groups remains poorly understood.

Just as the pattern and function of thermogenesis may vary between species, so can the mechanism of thermogenesis. Both the alternative oxidase (AOX) and plant uncoupling proteins (pUCPs) have been shown to be involved in thermogenic species of Araceae, each bypassing or uncoupling ATP synthesis from electron transport during respiration, with energy released as heat (Borecký and Vercesi, 2005; Watling *et al.*, 2008). In the limited number of species studied to date (including several Araceae), heat production is primarily via the alternative respiratory (AOX) pathway (Watling *et al.*, 2006; Grant *et al.*, 2008; Wagner *et al.*, 2008; Ito *et al.*, 2011; Miller *et al.*, 2011; Ito-Inaba *et al.*, 2019), whilst evidence for a role for pUCPs in thermogenesis is limited to the skunk cabbage (*Symplocarpus renifolius*) in which both AOX and pUCP may contribute to thermogenesis (Ito-Inaba *et al.*, 2008; Onda *et al.*, 2008). Little is known about the molecular basis of many floral traits relevant to pollinator attraction, including thermogenesis (Onda *et al.*, 2015), and the relevance of variation in thermal traits for different pollinators in mimetic systems.

The early diverging monocotyledon family Araceae is second to only Orchidaceae in the number of deceptive species (Renner, 2006; Chartier *et al.*, 2014). Within Araceae (approx. 140 genera and >3700 species), brood-site mimics are common, and most prevalent in the subfamily Aroideae and tribe Areae (Mayo *et al.*, 1997; Gibernau, 2011; Bröderbauer *et al.*, 2012; Nauheimer *et al.*, 2012; Chartier *et al.*, 2014; Boyce and Croat, 2018). Floral signals and traits within araceous and unrelated brood-site mimics have largely evolved to attract and retain two insect orders – Coleoptera and Diptera (Chartier *et al.*, 2014; Jürgens and Shuttleworth, 2015; Johnson and Schiestl, 2016). It is unclear if certain floral traits of brood-site mimics are associated with beetle or fly pollination in these systems. This may be due in part to a lack of information on effective pollinators in the majority of brood-site mimics, the tendency of studies to focus on specific floral traits in isolation (particularly floral scent) (Kite and Hetterscheid, 2017), floral trait complexity and the fact that some species are visited and/or pollinated by both orders (e.g. Quilichini *et al.*, 2010). Floral traits have been found to overlap between beetle- and fly-pollinated Araceae species across mixed pollination system types (Gibernau *et al.*, 2010); however, there is a lack of detailed comparative studies examining differences in brood-site mimics pollinated exclusively by these different insect orders, particularly at the intraspecific or congeneric level which can offer useful insight into evolutionary processes (Sayers *et al.*, 2020). Previous work has found that *Typhonium* (tribe Areae) are typically brood-site mimics, characterized by floral traps, the emission of strong fetid odours, floral thermogenesis, brief female and male phases of anthesis in protogynous inflorescences and visitation by both/either saprophagous beetles and flies (e.g. Cleghorn, 1914; Banerji, 1947; Sayers, 2019). There can, however, be significant variation in floral traits between *Typhonium* species which may reflect selection by different pollinator assemblages (Sayers *et al.*, 2020). In this study, we focus on two closely related *Typhonium* species, *T. angustilobum* and *T wilbertii*, which form a single monophyletic group and have similar geographical distributions in tropical Far North Queensland (FNQ) (Cusimano *et al.*, 2010; Hay, 2011), and were observed to be pollinated by different insect orders (Coleoptera and Diptera). We set out to (1) identify their pollinators; (2) compare the mechanism of thermogenesis and the genes involved; and (3) examine the floral traits, both sensory (i.e. thermogenic, olfactory and visual signals) and morphological, associated with pollinator divergence.

MATERIALS AND METHODS

Study sites and study species

Typhonium angustilobum F.Muell and *T. wilbertii* A.Hay share similar but allopatric distributions in FNQ, Australia (Fig. 1). *Typhonium wilbertii* is endemic to Australia whilst *T. angustilobum* also occurs in Southern New Guinea (Hay, 2011). *Typhonium angustilobum* was studied in a natural population at Shiptons Flat south of Cooktown (–15.79°, 145.24°) (on private land with open tropical woodland and cattle pasture), and in cultivation on private property on the Atherton Tablelands (plants sourced from Shiptons Flat) during February 2015–2017 (Fig. 1A). Two cultivated *T. angustilobum* sourced from populations in the Laura and Chillagoe regions in FNQ were also measured for anthesis and thermogenic patterns and floral morphology in 2018. *Typhonium wilbertii* was studied in a natural population at Macalister Range National Park at two adjacent sites (–16.6678°, 145.5668° and –16.6676°, 145.5662°) in the Wangetti coastal region (characterized by transitional wet sclerophyll forest, notophyll rainforest and open grassland), and in cultivation on the Atherton Tablelands (plants sourced from Turtle Cove, Macalister Range National

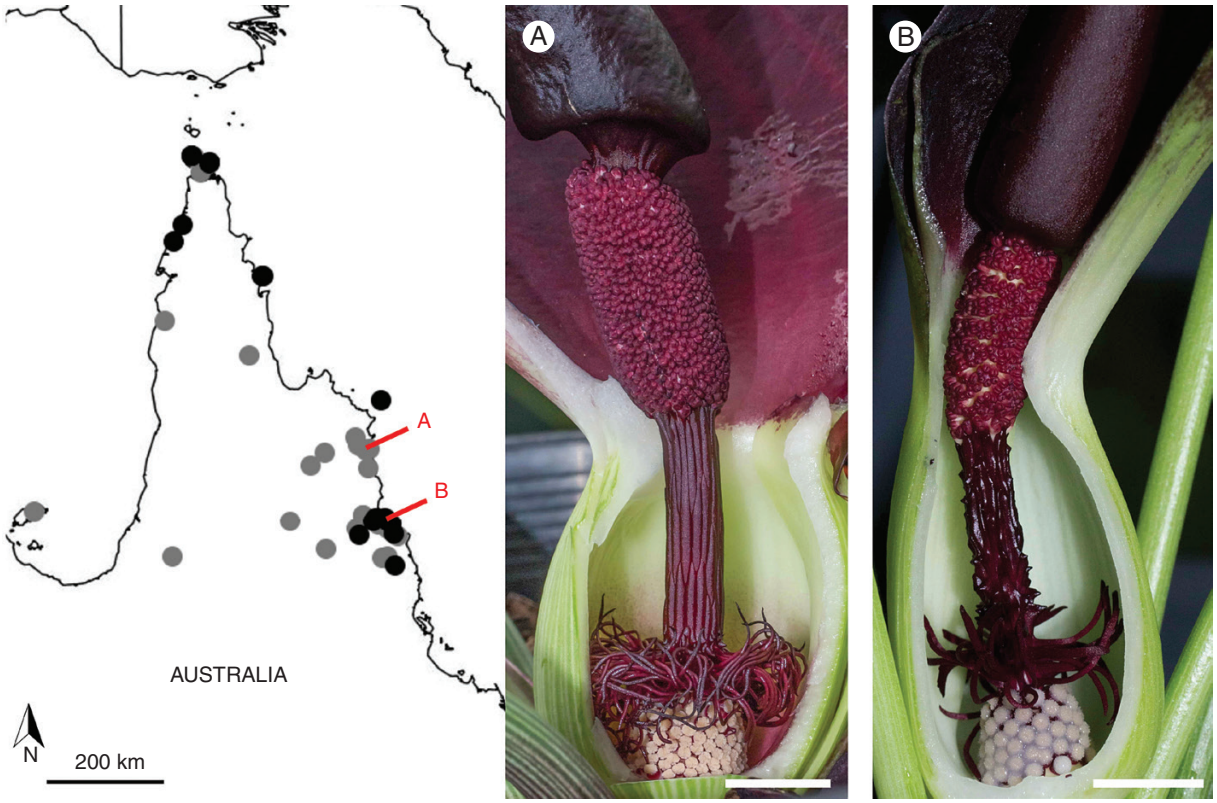

FIG. 1. Distribution of (A) *T. angustilobum* (grey) and (B) *T. wilbertii* (black) in Cape York Australia (Atlas of Living Australia). The location of the main source populations and study sites (A) Shiptons Flat and (B) Wangetti are labelled. Images show the reproductive organs of hermaphrodite inflorescences with the spathe partially removed (scale bar = 1 cm). Features shown are the spadix (surrounded by the spathe), comprised (from top to bottom) of the appendix, staminate zone above the spathe constriction, a sterile interstice with basal filiform organs and the pistillate zone at the base of the floral chamber (note the stigmatic fluid on the female florets of *T. wilbertii*).

Park –16.629°, 145.548°) during February 2016–2018 (Fig. 1B). Cultivated plants of both species were also studied at the University of Melbourne Burnley Campus from 2017 to 2019 (sourced from Shiptons Flat and Wangetti field populations). Voucher specimens from Shiptons Flat and Wangetti populations were lodged at the University of Melbourne Herbarium (*T. angustilobum* MELU M113406-7a, and *T. wilbertii* MELU M113409-10a).

Insect visitors and pollinators

Floral chambers from separate plants were sampled for trapped insects in the field during the late pistillate or early staminate stages of anthesis. Forty *T. angustilobum* inflorescences were sampled from a natural population at Shiptons Flat (n = 38) and in cultivation on the Atherton Tablelands (n = 2) in February 2015–2017, and 21 *T. wilbertii* inflorescences were sampled from natural populations at Wangetti (n = 17) and the same location in cultivation on the Atherton Tablelands (n = 4) in February 2016–2018. Two of the cultivated *T. wilbertii* inflorescences and one of the cultivated *T. angustilobum* inflorescences flowered within a 72 h window in February 2017 adjacent to one another. These inflorescences were sampled in the morning on Day 2 of anthesis and used to compare the trapping of insect taxa under spatially and temporally controlled common garden conditions. Assessments of the effectiveness of visiting insect families and species as pollinators were based on their relative abundance in floral chambers, observations of their morphological fit and behaviour in relation to reproductive organs and anthesis rhythms, and the presence of pollen attached to their bodies. Isolated inflorescences in cultivation at Burnley (*T. angustilobum* n = 3, *T. wilbertii* n = 7) were monitored for self-fertilization and compared with one hand-crossed inflorescence of each species to indicate their dependency on outcrossing for seed set.

Anthesis and thermogenic patterns

As for the majority of Aroideae, both species are perennial geophytes with short periods of plant growth and flowering during the tropical wet season (January–March). Multiple inflorescences were observed during anthesis (n = 28 *T. angustilobum*, n = 36 *T. wilbertii*) to identify the sequence of inflorescence development and the pattern of thermogenic activity. Floral temperature was measured by Extech SDL200 4-channel datalogging thermometers (TRIO Test and Measurement, Norwood, South Australia) using K-type thermocouple probes, placed 5 mm into the widest part of the appendix, the middle of the staminate zone and inside the floral chamber into the pistillate zone (n = 8 for both species). Ambient air temperature was measured and compared with that of the pistillate zone, which was determined to be

non-thermogenic. This non-thermogenic tissue was used as a baseline to quantify temperature increases in thermogenic tissues. Temperature recordings were taken at 10 min intervals and plants were shaded to negate the effect of intermittent direct solar radiation. A Fluke Ti95 thermal imager (Fluke Corp., Everett, WA, USA) monitored all floral organs during anthesis and provided infrared imagery during peak thermogenesis.

Molecular analyses of potential thermogenic pathways

Tissue sampling and RNA extraction. To investigate the pathway involved in heat generation, RNA was extracted from snap-frozen *T. angustilobum* and *T. wilbertii* inflorescences collected in the field and in cultivation (from Shiptons Flat and Wangetti, respectively), using the RNeasy kit (Qiagen, Germany). RNA was extracted from the thermogenic appendix and non-thermogenic female florets of inflorescences sampled during pre-thermogenic (1–2 d prior to the pistillate phase), thermogenic (during peak thermogenesis in the pistillate phase) and post-thermogenic (following pollen shed on Day 2) phases of anthesis. For each species, RNA was extracted from three independent biological replicates (inflorescences) collected during each stage of anthesis. cDNA was synthesized from (1 µg) RNA using SuperScript Iv VILO master mix (ThermoFischer).

Sequencing of Typhonium AOX cDNAs and AOX protein sequence analysis. To identify genes potentially involved in thermogenesis in *Typhonium*, BLAST searches of the onekp database (onekp.com) were undertaken using *Arum maculatum AOX1e* (AB565469.1) (Ito *et al.*, 2011), *Thaumatophyllum bipinnatifidum* (syn. *Philodendron bipinnatifidum*) *PbUCPa* (AB189674.1) and *Acorus americanus ACTIN* (Supplementary data Table S1). *Typhonium blumei* transcript sequences identified by BLAST searches were used to design primers (Supplementary data Table S1), tested for amplification of *T. angustilobum* and *T. wilbertii* cDNA, and validated by sequencing. As only a single, partial transcript sequence from *T. blumei* was identified in the onekp database for *AOX*, primers for amplification of the 5′ region of *AOX* were based on the *A. maculatum AOX1e* sequence.

Polymerase chain reactions using cDNA generated from the appendix and female florets of inflorescences during the thermogenic stage were used to amplify *AOX* and *UCP* DNA. The PCR products were cloned into pGEMT vectors (Promega), sequenced and used to assemble the *Typhonium* AOX sequences. Additional primers were designed to distinguish and extend *AOX1a* and *AOX1b* sequences (Supplementary data Table S1) (GenBank AOX accession numbers: *TaAOX1a* MN848524, *TaAOX1b* MN848525, *TwAOX1a* MN848526 and *TwAOX1b* MN848527). Multiple sequence alignments of the *Typhonium* AOX protein sequences and AOXs identified from thermogenic tissues of other species were performed using Clustal Omega via the European Bioinformatics Institute (EMBL-EBI) web interface, which also determined percentage identity.

Quantitative reverse transcription–PCR (RT–qPCR). Primers for RT–qPCR were designed based on the *T. blumei*, *T. angustilobum* and *T. wilbertii AOX* and *UCP* sequences (Supplementary data Table S1). Transcript levels of target genes were assessed using an absolute quantitative method with standard curves (Burton *et al.*, 2004, 2008), and normalized against the housekeeping gene *ACTIN* (Bustin, 2000). RT–qPCR was performed on three independent biological replicates for each of the three phases of anthesis (i.e. $n = 3$ inflorescences comprising the appendix and female florets) and samples were assayed in triplicate. Initial *AOX* primers were found to be specific for *AOX1b*, and a repeat experiment was performed to include *AOX1a* (resulting in six technical replicates for *AOX1b* and *UCP*). RT–qPCR was performed in a Quantstudio 5 Real-time PCR system (Applied Biosystems) using PowerUp SYBR green qPCR Master Mix (2X) in 10 µL reactions. The reaction was performed for 10 min at 95 °C followed by 40 cycles of 15 s at 95 °C and 1 min at 60 °C. Analysis was performed using QuantStudio Design and Analysis software v1.4.2.

Floral morphology and trapping mechanisms

Floral morphology and reflectance. Floral morphology was measured using a caliper and measuring tape to record the length and width (from the widest part) of reproductive zones, including the terminal appendix, staminate zone, pistillate zone and the spathe (Fig. 1). The angle of the spathe blade was measured from the vertical using a protractor during peak pistillate and staminate stages of anthesis ($n = 4$–25 for particular floral traits across species). An Ocean Optics Jaz fibre optic spectrophotometer, with PX lamp and fibre optic probe held at 45° to the spathe surface quantitated the central inner spathe colour of each species.

Scanning electron microscopy (SEM). A Leica M80 stereomicroscope with Leica IC80 HD camera (Leica Camera AG, Wetzlar, Germany) photographed epidermal features on the inner spathe of both species ($n = 3$) during the pistillate phase to confirm consistency in features across inflorescences of different plants. For SEM preparation, fresh tissue of one inflorescence of each species was dissected from (1) the lower spathe chamber; (2) the upper spathe chamber; (3) 1 cm above the spathe constriction; (4) the central spathe blade; and (5) the central part of the appendix (as described in Bröderbauer *et al.*, 2013; Sayers *et al.*, 2020). Male and female florets were also sampled for SEM, in addition to pollen grains and an individual *Philonthus* (Staphylinidae) (the most abundant visitor trapped by *T. angustilobum*) which were air-dried (SEM sample preparation and analysis details as in Sayers *et al.*, 2020).

Floral scent compounds

VOC sampling. Floral VOCs were sampled from intact inflorescences on separate plants – 12 *T. angustilobum* inflorescences from Shiptons flat, and nine *T. wilbertii* inflorescences from Wangetti and one from Turtle Cove. Floral VOCs were sampled between 17.00 and 19.30 h during the middle of the pistillate phase, signalled by a fully open inflorescence and enhanced insect attraction and scent emission. Supelco solid-phase microextraction (SPME) fibres (100 µm polydimethylsiloxane) were used to sample VOCs

as detailed in Sayers *et al.* (2020), due primarily to ease of use for remote fieldwork and reduced interference with the study system (Tholl *et al.*, 2006).

VOC analysis and identification. SPME fibres were thermally desorbed by gas chromatography (GC) and mass spectrometry (MS) using an Agilent technologies 7820A gas chromatogram with a Supelcowax10 polar column (30 m × 0.25 mm × 0.25 µm) coupled to an Agilent 5975 series single quadrupole mass spectrometer following methods described in Sayers *et al.* (2020). Peaks were integrated using Agilent Chemstation data analysis software. Relative amounts were calculated for each integrated VOC by dividing the absolute peak area by the sum of all VOC peak areas in the sample. The methods used to identify and shortlist VOCs are provided in Sayers *et al.* (2020). VOCs were classified according to structural groups following Knudsen *et al.* (2006).

Statistical analyses

Data analyses of floral traits and pollinators focused on comparing species, and the sampling of multiple populations was undertaken to ensure robust characterization. To compare insects trapped between species, insect count data were converted to mean (± s.e.) relative abundance of insect families. Independent sample *t*-tests tested for significant differences in floral traits between species (i.e. thermogenic and morphological data) in Minitab® Statistical Software (version 18; Minitab, Inc.). A two-way analysis of variance (ANOVA) tested for differences in *AOX* and *UCP* transcript expression with tissue type and anthesis stage in each species using JMP14 (SPSS software). Where there were significant tissue × stage interactions, one-way ANOVA tested for significant developmental differences in transcript expression in each floral tissue. Data were log or square root transformed when they did not meet assumptions of normal distribution and variance homogeneity, tested using Shapiro–Wilk and Levene tests, respectively. Tukey HSD post-hoc tests were applied to identify differences between stages and tissues at $P < 0.05$. Scent analysis was undertaken using VOC presence/absence and square root transformed relative amount data (i.e. percentage composition), based on the Sørensen and Bray–Curtis similarity indices, respectively (excluding minor pooled unknowns). Percentage composition data were square root transformed to lessen the impact of the most abundant VOCs. A one-way analysis of similarity (ANOSIM) using 10 000 permutations was applied to VOC presence/absence data to test for a significant difference in scent composition between species (in PRIMER 7.0.13). An *R* value of 1 indicates complete separation between groups, whilst a value of zero indicates no separation (Clarke and Gorley, 2015). When ANOSIM indicated a significant difference, similarity percentage analysis (SIMPER) was conducted to assess the average dissimilarity of samples within and between species and to identify the average contribution of individual compounds (Clarke and Gorley, 2015). SIMPER was applied to square root-transformed percentage composition data.

RESULTS

Insect pollinators

Floral chambers of *T. angustilobum* inflorescences accumulated and trapped a total of 1832 Coleoptera and five Diptera (Table 1) across 40 inflorescences (at natural and cultivated sites combined) during the pistillate phase of anthesis. Within the Coleoptera, Staphylinidae belonging to four subfamilies accounted on average for 57.3 % of insects caught per inflorescence (Fig. 2); other abundant Coleoptera trapped were Hydrophilidae, Scarabaeidae and Ptiliidae. Conversely, *T. wilbertii* trapped a total of 570 Diptera and 80 Coleoptera (Table 1) across 21 inflorescences (natural and cultivated). Diptera accounted for 81 % of trapped insects per inflorescence, with families in the late diverging section Schizophora (e.g. Sphaeroceridae and Sepsidae) accounting for 88.2 % of flies trapped (Table 1; Fig. 2). The average catch rates were 46.9 (± s.e. 7.8) and 31.0 (± s.e. 7.3) insects per inflorescence for *T. angustilobum* and *T. wilbertii*, respectively. Insect taxa trapped were consistent between natural and cultivated populations for each species and, similarly, in the common garden setting, *T. angustilobum* (163 Coleoptera) and *T. wilbertii* (131 Diptera and 13 Coleoptera) trapped divergent insect assemblages (Table 1; Fig. 2).

Staphylinidae were frequently observed slipping into the floral chamber of *T. angustilobum* during the pistillate stage of anthesis (Fig. 3). The steep floral chamber walls and small confines of the chamber made it difficult for Staphylinidae to escape. Numerous flies (e.g. Sphaeroceridae, Sepsidae and Calliphoridae) congregated on *T. angustilobum* inflorescences, but were rarely observed entering the floral chamber (Fig. 3B, C). Staphylinidae, in addition to trapped Hydrophilidae and the introduced *Aphodius lividus* (Scarabaeidae), left the floral chamber during pollen shed using the spadix as a ladder to exit the chamber and accumulating large pollen loads (Fig. 3E, F, H). Sphaeroceridae and Sepsidae were observed entering the floral chamber of *T. wilbertii* during the pistillate stage (Fig. 4). Large flies were attracted, including Calliphoridae (Fig. 4C), but were generally too large to enter the *T. wilbertii* floral chamber, and Coleoptera were rarely observed visiting inflorescences. Unlike Coleoptera, Diptera landed on the spathe or appendix in a controlled manner and were drawn towards the chamber entrance where they slipped into the *T. wilbertii* chamber (Fig. 4E, F). During pollen shed, trapped Diptera (particularly Sphaeroceridae) used the spadix to exit the chamber through the narrow spathe constriction (Fig. 4G), contacting pollen (Fig. 4H, I). Combined, our observations and the relative abundance of insects trapped in close proximity to female florets during anthesis (Table 1; Fig. 2) strongly indicated that Staphylinidae (particularly *Philonthus* sp.), and Hydrophilidae (Megasternini) and *A. lividus* were primary and secondary pollinators of *T. angustilobum*, respectively. In contrast, Sphaeroceridae, and other fly families such as Sepsidae (and potentially staphylinid beetles), trapped in lower abundances, were considered primary and secondary pollinators of *T. wilbertii*, respectively.

There was no evidence of oviposition and egg or larvae development in the inflorescences of either species. The Shiptons Flat population comprised >30 fertilized *T. angustilobum*

TABLE 1. *Total number of insect taxa trapped in* T. angustilobum *and* T. wilbertii *inflorescences identified to the lowest taxonomic level possible showing numbers trapped in inflorescences at natural and cultivated (in parentheses) sites*

		T. angustilobum		*T. wilbertii*	
Sub-order	Insect family	*n* = 38 (*n* = 2)	**Total**	*n* = 17 (*n* = 4)	**Total**
Coleoptera		**1541 (291)**	**1832**	**66 (14)**	**80**
Polyphaga					
	Staphylinidae				
	Staphylininae				
	Staphylinini				
	Philonthus sp.	467 (90)[64]	557	11 (1)[1]	12
	Xantholinini				
	sp. 1	34 (15)[1]	49	1 (0)	1
	sp. 2	0 (6)[1]	6		
	Aleocharinae	231 (3)[1]	234	25 (0)	25
	Oxytelinae				
	Oxytelini			2 (0)	2
	Anotylus sp.	54 (17)[5]	71	1 (0)	1
	Oxytelus sp.	5 (3)[3]	8	7 (0)	7
	Paederinae				
	Lithocharis sp.	60 (3)[3]	63	4 (0)	4
	Hydrophilidae			2 (0)	2
	Megasternini	410 (80)[76]	490	3 (8)[8]	11
	Scarabaeoidea				
	Aphodiinae				
	Aphodius lividus	231 (68)[3]	299	2 (4)[4]	6
	Trogidae			2 (0)	2
	Scarabaeinae			1 (0)	1
	Ptiliidae	47 (6)[6]	53	5 (1)	6
	Leiodidae	1 (0)	1		
	Chrysomelidae	1 (0)	1		
Diptera		**5 (0)**	**5**	**244 (326)**	**570**
Brachycera					
	Hybotidae				
	Tachydromiinae			26 (0)	26
Schizophora					
Acalyptratae					
	Sphaeroceridae	5 (0)	5	118 (306)[125]	424
	Sepsidae			55 (5)[3]	60
	Drosophilidae			0 (13)[2]	13
Calyptratae					
	Calliphoridae			5 (1)[1]	6
Nematocera					
	Psychodidae			40 (1)	41
Total			**1837**		**650**

Superscripts show the number of each taxa trapped in a sub-set of inflorescences in cultivation which were sampled under common garden conditions.

inflorescences in February 2016. Some plants retained three or more fertilized inflorescences, and seed aggregates were still housed inside the floral chamber (Fig. 3I, J). Seed set at the *T. wilbertii* Wangetti population was observed between April and July 2017 (D. Baume, pers. comm. 18 July 2017); fruit similarly developed inside the floral chamber, with some plants retaining multiple fertilized inflorescences (Fig. 4J, K). No unmanipulated inflorescences in cultivation at Burnley self-pollinated, whilst one hand-crossed inflorescence of each species set fruit.

Anthesis rhythms and thermogenic patterns

Anthesis rhythms were very similar for both protogynous species and lasted approx. 36 h over two consecutive days, Day 1 and Day 2 marking the pistillate and staminate phases, respectively (Fig. 5). On Day 1 of anthesis, inflorescences gradually opened throughout the afternoon and were fully open by the evening (approx. 12.00–18.00 h, Fig. 5). Transient thermogenesis was detected in the appendices and to a lesser extent in the staminate zones, but not in female florets or sterile zones. Major thermogenic activity was recorded in the appendices of both species at dusk, coinciding with enhanced scent release and insect attraction (Fig. 5). There was no significant difference in peak temperature increase (11.3 ± 3.3 °C and 11.4 ± 2.0 °C for *T. angustilobum* and *T. wilbertii* appendices, respectively), absolute peak temperature above non-thermogenic tissue or the timing and duration of elevated appendix temperatures between species (Table 2). Inflorescences continued to attract pollinators after dusk as the spathe gradually constricted around the base of the staminate zone, arresting insects overnight in perfect traps (i.e. insects are denied egress until pollen shed) (Fig. 5). Staminate zone temperatures of both species were modestly elevated through the night (Fig. 5). The *T. angustilobum* staminate zone maintained a temperature of approx. 2 °C above that of

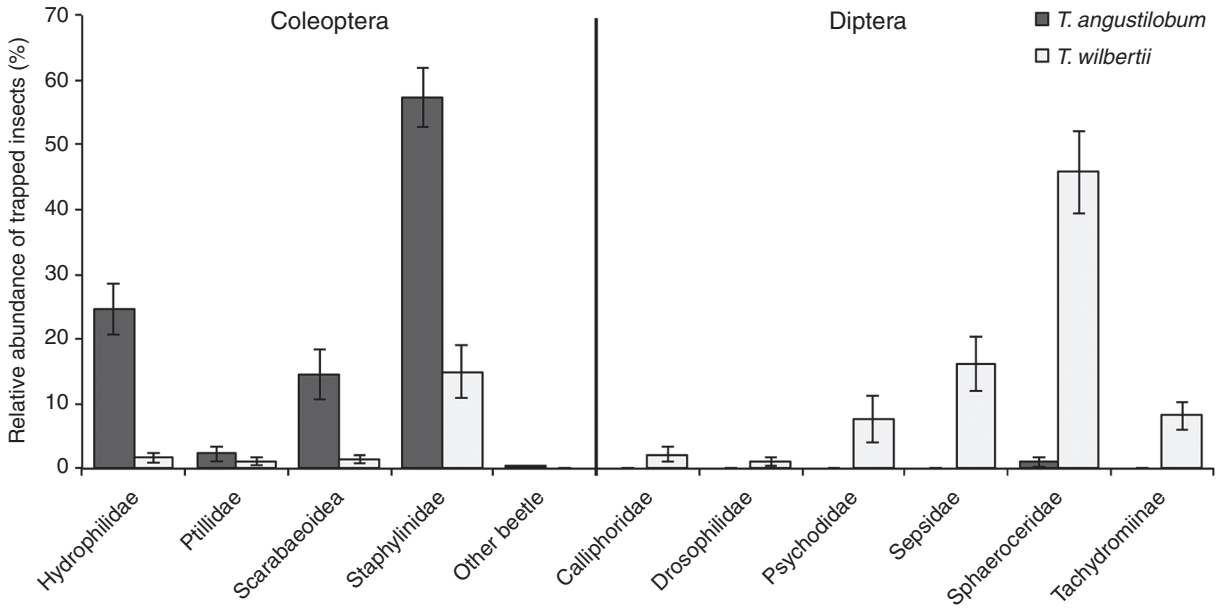

FIG. 2. Mean (± s.e.) relative abundance of coleopteran and dipteran insect families trapped in *T. angustilobum* ($n = 40$) and *T. wilbertii* ($n = 21$) inflorescences across both natural and cultivated sites. Refer to Table 1 for more detailed classifications of insect taxa.

non-thermogenic tissue until a distinct peak at around 18.00 h (5.9 ± 2.5 °C above non-thermogenic tissue) in the evening on Day 2 which initiated during the onset of pollen shed in the mid to late afternoon (Fig. 5A). The temperature of the staminate zone of *T. wilbertii* was approx. 1 °C above that of the non-thermogenic tissue through the night until pollen shed in the mid to late late afternoon on Day 2 (Fig. 5B).

Heating pathways: tissue- and stage-specific AOX and UCP expression

To investigate the pathways leading to heating in *T. angustilobum* and *T. wilbertii*, transcripts of *AOX* and *pUCP* genes were investigated in the appendices and non-thermogenic female florets at pre-thermogenic, thermogenic and post-thermogenic stages of anthesis. Two different *AOX* sequences were identified from both species, indicating the presence of at least two AOX isoforms, designated *TaAOX1a* and *TaAOX1b* from *T. angustilobum* and *TwAOX1a* and *TwAOX1b* from *T. wilbertii*. In both species, expression of both *AOX* transcripts was significantly higher in thermogenic appendices than in non-thermogenic female florets (significant main effect tissue, two-way ANOVA $P < 0.05$), and remained low in female florets during anthesis, with no significant stage-specific variation (Fig. 6). In both species, *AOX1a* and *AOX1b* transcript expression was highest in the thermogenic appendices and decreased significantly post-thermogenesis (Fig. 6). The increase in *AOX1b* expression in the appendix between pre-thermogenic and thermogenic stages was also significant for *T. wilbertii* (Fig. 6B). *AOX1b* expression was 7.3- and 2.6-fold higher than *AOX1a* expression in thermogenic appendices of *T. angustilobum* and *T. wilbertii*, respectively. In contrast, *pUCP* transcript expression was relatively low and similar in the appendix and female florets of both species, and no significant increase at the thermogenic stage was detected (Fig. 6A, B).

Alignment of the partial deduced amino acid sequences of *Typhonium* AOXs revealed that the two AOX1a proteins shared 98.40 % identity, and the AOX1b proteins shared 97.06 % identity, both higher than the shared identity of AOX1 sequences within species (Supplementary data Fig. S1). AOX1a and AOX1b proteins shared the highest identity with different AOX proteins from other thermogenic taxa (Supplementary data Fig. S1B). Both *T. wilbertii* AOX proteins and TaAOX1b contained structural features of typical plant AOXs (Berthold *et al.*, 2000), including two regulatory cysteine residues (CysI and CysII), four α-helical bundles and six ligands for iron atoms at the catalytic centre (Fig. 6C; Supplementary data Fig. S2). The least complete TaAOX1a sequence also contained CysI and CysII, but did not cover the fourth α-helix or two ligands (Supplementary data Fig. S2). Three of four potential regulatory regions within AOX proteins (Crichton *et al.*, 2005) were sequenced in all except TaAOX1a (Fig. 6C). *Typhonium* AOXs were similar and relatively well conserved in regions 1 and 2, but differed in region 3, which has been shown to relate to the responsiveness to α-keto acids (e.g. pyruvate) (Crichton *et al.*, 2005; Ito *et al.*, 2011). Both TaAOX1b and TwAOX1b contained an ENV motif in region 3, typical of AOXs activated by pyruvate (Onda *et al.*, 2007; Ito *et al.*, 2011), whereas TwAOX1a contained QDT, similar to AOXs known to be insensitive to activation by pyruvate (Crichton *et al.*, 2005; Ito *et al.*, 2011).

Floral morphology and trapping mechanisms

All inflorescence dimensions, apart from the length of the pistillate zone, were significantly larger in *T. angustilobum* than in *T. wilbertii* (Table 3). The average spathe blade angle from the vertical increased from the pistillate to staminate stage of anthesis in both species; however, the spathe angle during both phases was significantly steeper in fly-pollinated

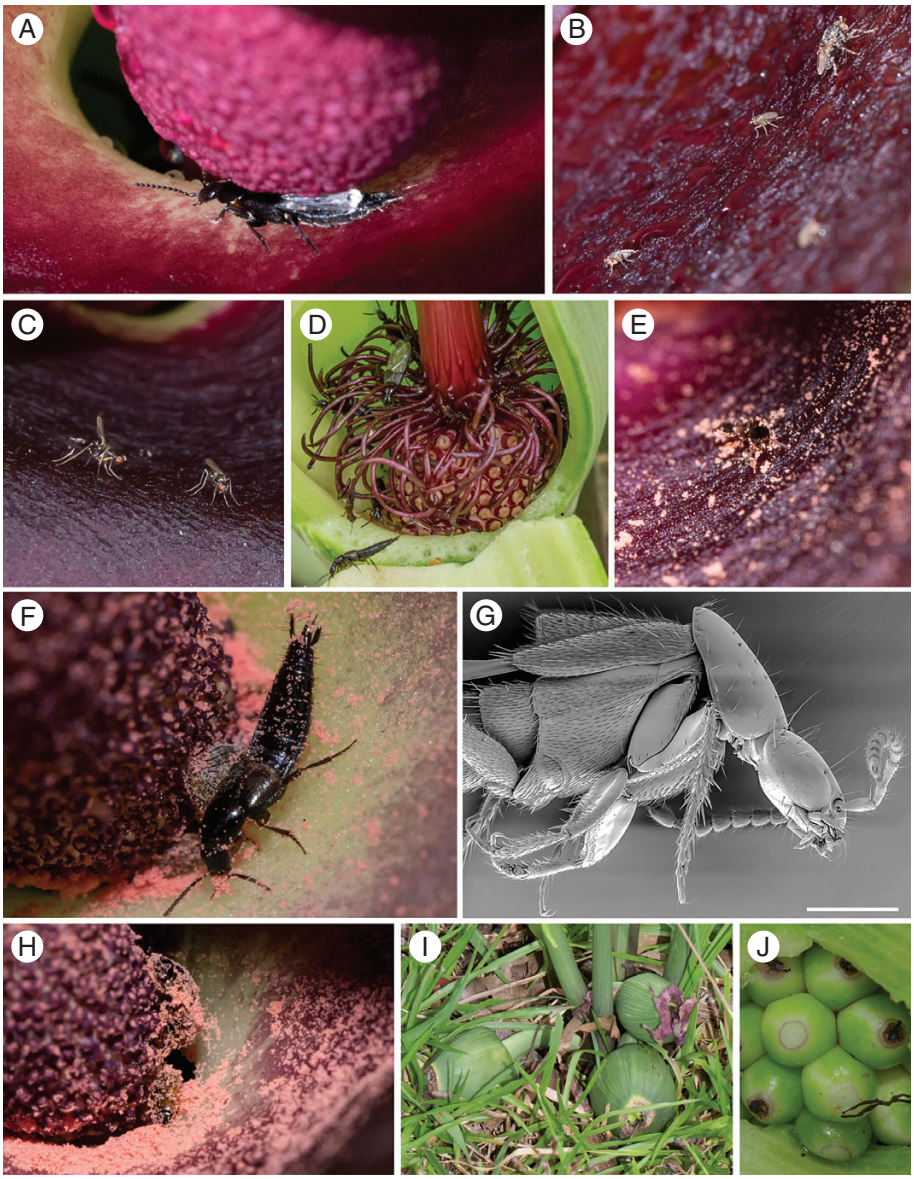

FIG. 3. *Typhonium angustilobum*–insect interactions: (A) *Philonthus* sp. at the floral chamber entrance during the pistillate phase of anthesis; (B, C) Sphaeroceridae and Sepsidae congregating on the spathe; (D) Staphylinidae trapped in the floral chamber amongst sterile filiform organs on the morning of Day 2 visible after removing the chamber wall; (E) *Xantholinini* sp.1 leaving the inflorescence with pollen adhered; (F) *Philonthus* sp. brushing past the male florets with pollen adhered; (G) SEM image of *Philonthus* sp. showing the microscopic hairs covering the thorax, legs and head (scale bar = 500 µm); (H) Megasternini and *Aphodius lividus* (above) leaving the floral chamber with pollen adhered; (I, J) fertilized inflorescences with seed aggregates still housed inside the floral chamber.

T. wilbertii than in beetle-pollinated *T. angustilobum* (Table 3). The spathe constriction around *T. wilbertii* spadices was tighter compared with *T. angustilobum*, particularly during the staminate stage, and the more constricted morphology extended up the *T. wilbertii* spathe (Fig. 5B). Spathe colour was comparable between species (percentage reflectance increased at similar rates above 600 nm, Supplementary data Fig. S3), each characterized by a burgundy spathe and appendix. The burgundy coloration transitioned sharply to green at the floral chamber entrance (more prominent in *T. wilbertii*), making the entrance to the floral chamber brighter than the surrounding spathe (Fig. 5). Spadices of both species have sterile filiform organs directly above the pistillate zone in the floral chamber (Fig. 1), with the sterile interstice above these hairs naked in *T. angustilobum* but comprised of some smaller papillate sterile organs in *T. wilbertii* (Fig. 1).

The morphology and basal area of raised cells on the inner spathe epidermis differed between species. In *T. angustilobum*, the central spathe epidermis comprised densely packed and raised tabular cells from approx. 1 cm above the spathe constriction (Fig. 7A, B). In contrast, the central spathe of *T. wilbertii* featured less densely packed and more prominent downward pointing papillae, approximately half the basal area of the *T. angustilobum* tabular cells (Table 3), and these papillae continued down the lower spathe epidermis to the spathe constriction in *T. wilbertii* (Fig. 7C). Curved or raised cells were absent in the floral chamber in both species (Fig. 7D), and the appendix epidermis in both

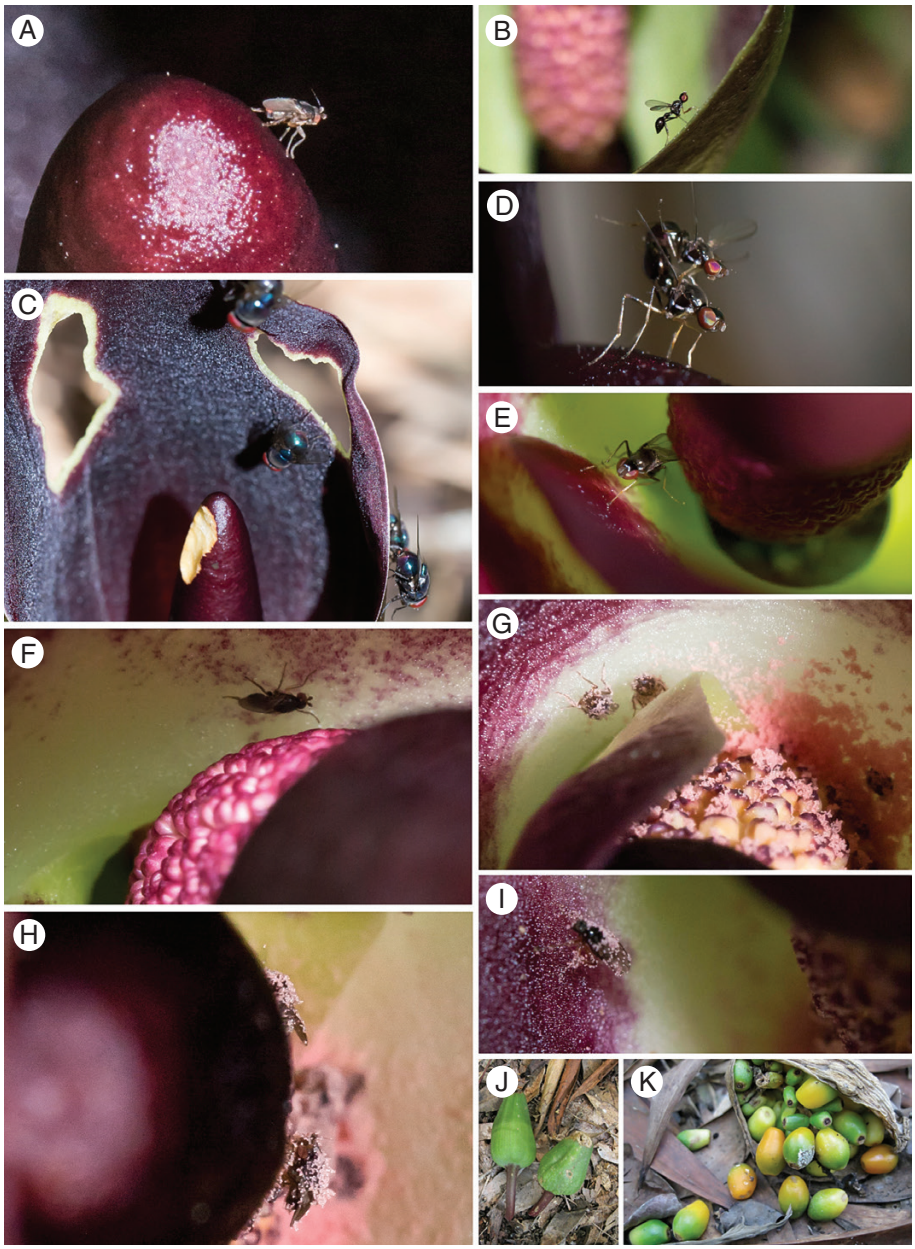

FIG. 4. *Typhonium wilbertii*–insect interactions: (A, B) Sphaeroceridae and Sepsidae attracted to *T. wilbertii* during the pistillate phase of anthesis; (C) Calliphoridae congregating on the spathe; (D) Sepsidae copulating on the inflorescence; (E, F) Diptera (Sepsidae and Sphaeroceridae) slipping down the steep waxy spathe towards the floral chamber entrance; (G, H) Sphaeroceridae leaving the floral chamber during the staminate phase of anthesis with pollen adhered; (I) Tachydromiinae leaving with pollen adhered; (J, K) fertilized inflorescences with seed aggregates still housed inside the floral chamber until maturation (images J and K by D. Baume).

species comprised flat tabular cells interspersed with stomata. Some differences in pollen grain morphology, and male and female floret morphology between species, were observed, including the presence of stigmatic fluid extruded from *T. wilbertii* stigmas following the peak pistillate phase of anthesis which was not discernible on the stigmas of *T. angustilobum* during anthesis (Fig. 7E–H).

Floral scent compounds

Typhonium angustilobum emitted a pungent acrid odour, whilst *T. wilbertii* emitted a dung-like odour, with sweet and floral components. This was reflected in differences in the total of 57 VOCs identified across both species (Table 4). *Typhonium angustilobum* and *T. wilbertii* contained a total of 37 and 35 VOCs, respectively, of which 15 were recorded in both species. The majority of shared compounds, however, occurred in less than half of *T. wilbertii* samples and were mainly sesquiterpenes. In addition, the relative amounts of VOCs common to both species differed. For example, whereas *p*-cresol and skatole made up 3 and 24 % of total VOC peak area in *T. wilbertii*, respectively, they were either detected at low levels or not detected at all in *T. angustilobum* inflorescences. ANOSIM confirmed significant differences in the

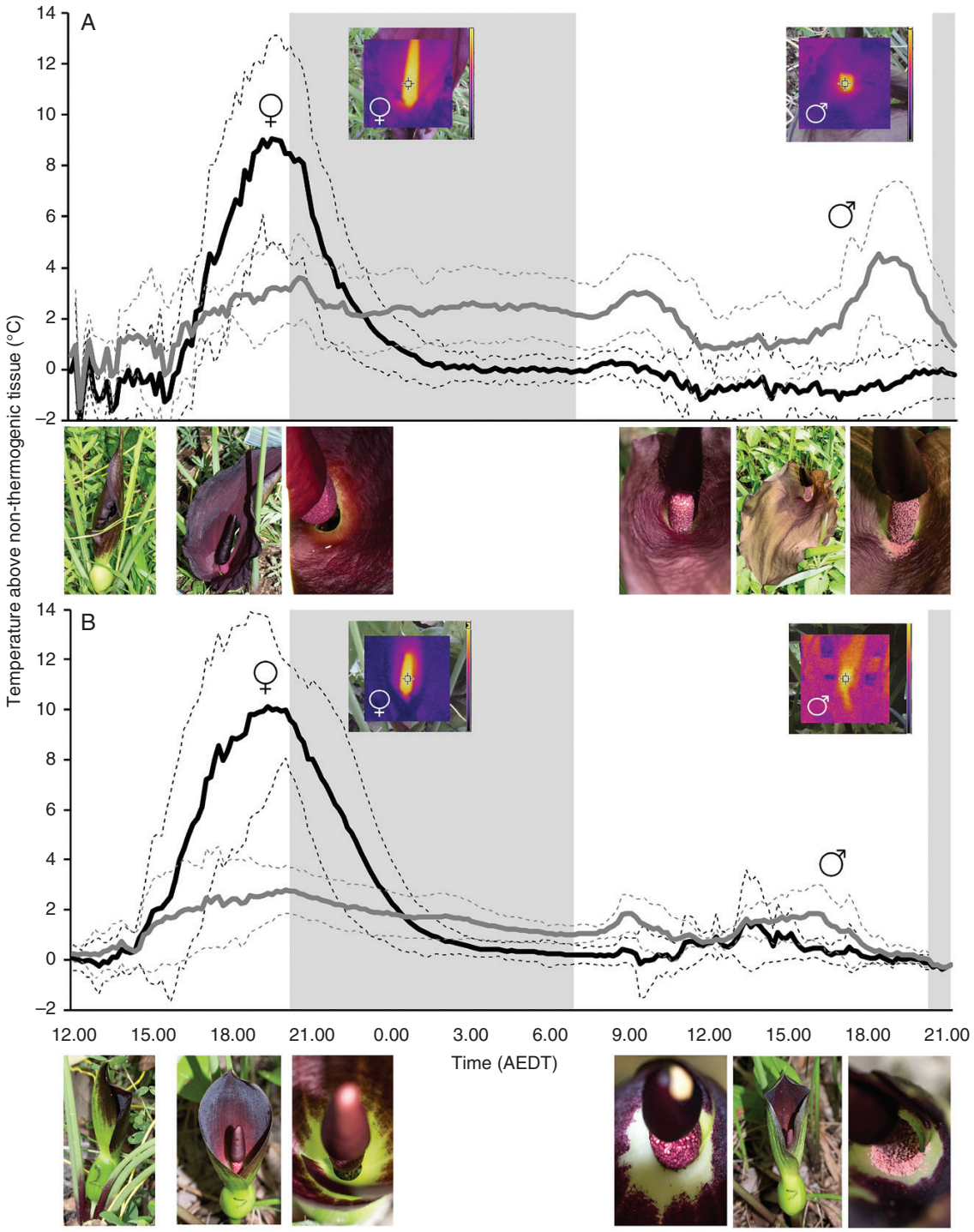

FIG. 5. Anthesis and thermogenic patterns of (A) *T. angustilobum* and (B) *T. wilbertii*. Temperature traces (mean ± s.d.) of *T. angustilobum* and *T. wilbertii* show temperature increases in the appendix (solid black line) and staminate zone (solid grey line) relative to non-thermogenic tissue (dashed lines show the standard deviation from the mean). The period between last and first light is shaded light grey, and the female and male symbols signal the timing of peak thermogenesis and onset of pollen shed, respectively. Infrared images correspond to peak temperature increases in the appendix and staminate zone during the pistillate and staminate phases of anthesis, respectively, and images of floral development and spathe behaviour correspond approximately to the time of day on the *x*-axis (AEDT = Australian Eastern Daylight Saving Time).

presence and absence of VOCs between species (ANOSIM species $R = 1$, $P \leq 0.0001$), and SIMPER analysis showed an average similarity of 11.7 % between species, with the compounds bicyclogermacrene and skatole contributing most to the dissimilarity. The average similarity amongst inflorescences of each species was 86.9 % for *T. angustilobum* and 72.6 % for *T. wilbertii*. *Typhonium angustilobum* samples were characterized by high relative amounts of bicyclogermacrene, elemene

TABLE 2. *Anthesis and thermogenic patterns (mean ± s.d.) of the appendices in* T. angustilobum *and* T. wilbertii

	T. angustilobum	*T. wilbertii*	(d.f.) *t*-value	*P*-value
Anthesis	*n* = 28 (3)	*n* = 36 (2)		
Peak pistillate (Day 1)	Evening	Evening		
Staminate onset (Day 2)	14.00–17.00 h	14.00–17.00 h		
Thermogenesis (pistillate stage)	*n* = 8 (3)	*n* = 8 (2)		
Peak temperature increase range above ntt (°C)	7.3–15.3	8.1–14.5		
Peak temperature increase above ntt (°C)	11.3 ± 3.3	11.4 ± 2.0	(14) –0.14	0.893
Absolute peak temperature (°C)	36.4 ± 2.0	38.7 ± 2.5	(14) –2.07	0.057
Time of peak temperature increase (h:min)	19:15 ± 1:05	19:00 ± 1:05	(14) 0.42	0.681
Time temperature increase starts (h:min)	15:55 ± 1:25	15:10 ± 1:45†	(12) 0.84	0.418
Time elevated temperature ends (h:min)	0:20 ± 1:55	1:25 ± 1:05†	(12) –1.27	0.227
Duration of elevated temperature (min)	507 ± 134	617 ± 127†	(12) –1.56	0.146

The peak pistillate stage and staminate onset are defined as the period of enhanced insect attraction and thermogenic activity, and the onset of pollen shed, respectively (*n* = number of inflorescences observed/measured, number of populations within parentheses; ntt = non-thermogenic tissue).

Results of independent samples *t*-tests.

†Data derived from sample size of *n* = 6, due to sampling of incomplete temperature traces for some inflorescences.

isomer, β-gurjunene, β-elemene, pentadecane, aristolene, viridiflorene and δ-elemene, explaining 66.3 % of the similarity among samples. *Typhonium wilbertii* samples were characterized by skatole, pentadecane, capparatriene, β-ionone, (2*Z*,4*E*)-3,7,11-trimethyl-2,4-dodecadiene, dihydro-β-ionone, *p*-cresol and 2-pentadecanone, explaining 66.9 % of the similarity among samples (Fig. 8, Table 4).

DISCUSSION

We confirm that *T. angustilobum* and *T. wilbertii* are brood-site mimics, functionally specialized (Fenster *et al.*, 2004) to deceive saprophagous beetle and fly pollinator assemblages, respectively. Both species were very similar in spathe colour, the pattern of anthesis, and the timing, intensity, duration and mechanism of floral thermogenesis, and shared highly homologous AOX proteins. In contrast, there were marked differences in scent between *T. angustilobum* and *T. wilbertii*, suggesting that scent is the most important signal to attract divergent insect pollinators in these brood-site mimetic systems. Significant variation in their spathe morphology suggests that once insects are attracted to an inflorescence, floral morphology and trapping mechanisms are also critical for the filtering of the two insect orders.

Functional specialization to different pollinator groups

Typhonium angustilobum almost exclusively trapped more ancestral Coleoptera, namely the families Staphylinidae, Hydrophilidae and Scarabaeidae, which form part of a clade that diversified from the mid Mesozoic (McKenna *et al.*, 2019). These families are known to visit and pollinate other araceous species including brood-site mimics, and mutualistic systems including many thermogenic species (Pellmyr and Patt, 1986; Sivadasan and Kavalan, 2005; Hoe *et al.*, 2018; Moretto *et al.*, 2019; Sayers *et al.*, 2019, 2020). All abundant beetle families trapped were considered effective pollinators, although Staphylinidae and particularly *Philonthus* sp. were considered most effective due to their abundance, moderate size and hairiness (Fig. 3F, G) (Stavert *et al.*, 2016). Staphylinidae are known for their predacious and saprophagous habits (Davis, 1994; Thayer, 2016), and *Philonthus* are known to visit decomposing substrates to prey on insects and their eggs and larvae (Hu and Frank, 1997; Walsh and Posse, 2003). Hydrophilidae (Sphaeridiinae: Megasternini), also known for their saprophagous or coprophagous habit, are commonly found in decaying plant material, dung and carrion (Campbell, 1976; Davis, 1994; Lawrence and Ślipiński, 2013; Arriaga-Varela *et al.*, 2018). The introduced *Aphodius lividus* (Stebnicka and Howden, 1995) was the only Scarabaeidae trapped in *T. angustilobum* and, though it may act as an effective pollinator of *T. angustilobum* (Fig. 3H), floral traits would not have evolved in association with this species.

Typhonium wilbertii trapped an array of Diptera and Coleoptera, though only Diptera, particularly higher Acalyptratae fly families Sphaeroceridae and Sepsidae (which diversified during the Paleogene; Wiegmann *et al.*, 2011) and to a lesser extent Psychodidae, were considered effective pollinators due to their relative high abundance in *T. wilbertii* floral chambers (Figs 2 and 4G, H). We suggest that floral traits of *T. angustilobum* are more ancestral since pollination by higher flies is a more recent insect–plant association than pollination by beetles. Saprophagous or coprophagous Sphaeroceridae and Psychodidae, common dung-inhabiting families (Campbell, 1976; Bishop *et al.*, 1998), are known pollinators of other araceous brood-site mimics, particularly thermogenic *Arum* species (e.g. Kite *et al.*, 1998; Albre *et al.*, 2003; Quilichini *et al.*, 2010; Urru *et al.*, 2010). The insects trapped were not typically anthophilous and, also unlike mutualistic brood-site pollination (Chartier *et al.*, 2014), there was no evidence of insect egg or larvae development in inflorescences. Further, stigmatic fluid secreted by *T. wilbertii* was not an obvious nutritional reward involved in the attraction of pollinators since it was not present until after the peak pistillate phase of anthesis. We therefore hypothesize that *T. angustilobum* and *T. wilbertii* have evolved to exploit the pre-existing sensory biases of diverse suites of insects (Schiestl and Dötterl, 2012; Schiestl, 2017) through a form of deceptive floral mimicry of cues used by insects to find decomposing substrates that provide sites for oviposition, mating, feeding and/or host/prey location. Whether

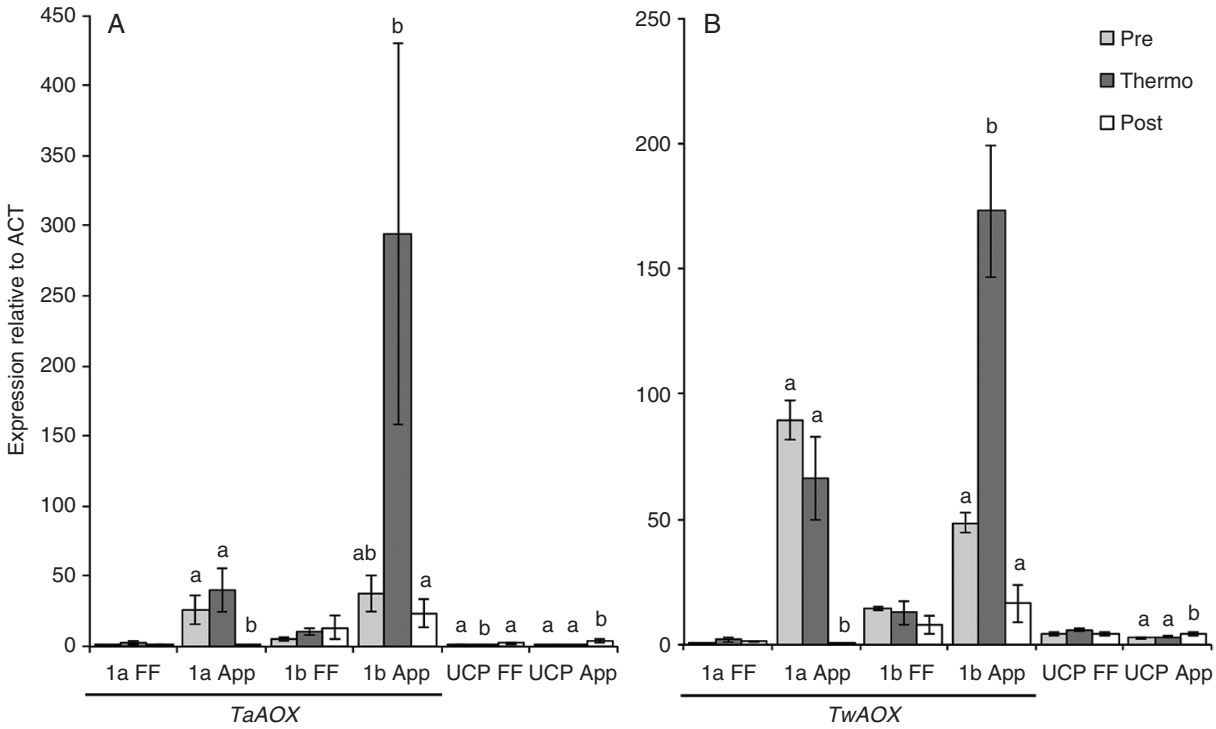

C

	Region 1		Region 2	Region 3
AmAOX1a*	SYWGV	RWT**C**FR	RYG**C**RA	I**ENV**PA
AcoAOX1a	SYWGV	RWT**C**FR	RYA**C**RA	I**ENV**PA
SrAOX1*	SHWGI	RWS**C**FR	RYG**C**RA	I**ENV**PA
TaAOX1b	SYWGV	RWA**C**FR	RYG**C**RA	I**ENV**PA
AmAOX1b*	SYWGV	RWT**C**FR	RYG**C**RA	I**ENV**PA
TwAOX1b	SYWGV	RWA**C**FR	RYG**C**RA	I**ENV**PA
PbAOX	SYWDV	RWA**C**FR	RYA**C**RA	I**KNV**PA
NnAOX1b^	SYWGL	RWN**S**FR	RYG**C**RA	I**ENV**PA
NnAOX1a^	SYWGM	KWN**S**FR	RYG**C**RA	I**QNV**PA
CrAOX1	-----	PWN**S**FR	RYG**C**RA	I**PNV**PA
DvAOX	SYWGV	RWT**C**FR	RYA**C**RA	I**QDS**PA
AmAOX1e#	SYWGV	RWT**C**FR	RYA**C**RA	I**QNT**PA
AmAOX1g#	SYWGV	RWT**C**FR	RYA**C**RA	I**QDT**PA
AcoAOX1b	SYWGV	RWT**C**FR	RYA**C**RA	I**QDT**PA
TwAOX1a	SYWGV	RWT**C**FR	RYA**C**RA	I**QDT**PA
TaAOX1a	SYWGV	RWT**C**FR	RYA**C**RA	
SvAOX1#	SYWAV	RWT**C**FR	RYA**C**RA	I**QDC**PA

FIG. 6. Expression levels (mean ± s.e., $n = 3$) of *AOX* and *pUCP* transcripts in (A) *T. angustilobum* and (B) *T. wilbertii* non-thermogenic female florets (FF) and thermogenic appendices (App), across three phases of anthesis. Different letters indicate significant differences in transcript expression levels between the phases of anthesis (within each tissue) at $P < 0.05$. The appendices of the three inflorescences sampled during the thermogenic stage were on average 10.7 °C (± s.d. 3.1) and 15.6 °C (± s.d. 2.3) above ambient for *T. angustilobum* and *T. wilbertii*, respectively. (C) Comparison of deduced amino acid sequences of *T. wilbertii* and *T. angustilobum* AOX proteins with previously reported AOXs from thermogenic tissues. Sequence alignment of three of four possible regions proposed to influence AOX regulation by Crichton *et al.* (2005) (NB: TaAOX1a partial sequence did not capture region 3; region 4 was not captured in any partial *Typhonium* sequences). Amino acids shaded in grey have potential involvement in AOX regulation, with those highlighted in yellow likely to be related to activation by α-keto

Table 3. *Floral organ measurements – spathe and spadix dimensions, spathe angle relative to vertical and basal area of spathe papillate cells – of* T. angustilobum *and* T. wilbertii *inflorescences (mean ± s.d. of* n *replicates)*

	T. angustilobum		*T. wilbertii*		(d.f.) *t*-value	*P*-value
		n		*n*		
Spadix length (cm)	13.1 ± 2.5	15	8.6 ± 0.9	25	(38) 8.66	0.001***
Appendix length (cm)	7.4 ± 1.5	15	3.2 ± 0.7	25	(38) 12.58	0.001***
Appendix width (cm)	1.7 ± 0.3	15	1.0 ± 0.3	25	(38) 7.53	0.001***
Staminate zone length (cm)	2.5 ± 0.4	15	1.9 ± 0.2	25	(38) 6.33	0.001***
Staminate zone width (cm)	1.1 ± 0.2	15	0.7 ± 0.2	25	(38) 7.32	0.001***
Pistillate zone length (cm)	1.0 ± 0.1	15	0.9 ± 0.1	25	(38) 1.31	0.198
Pistillate zone width (cm)	1.2 ± 0.1	15	0.9 ± 0.1	25	(38) 6.17	0.001***
Spathe length (cm)	17.4 ± 3.6	14	9.7 ± 2.0	12	(24) 6.56	0.001***
Spathe width (cm)	12.7 ± 1.8	14	7.2 ± 1.4	12	(24) 8.54	0.001***
Spathe angle PA (°)	38.0 ± 4.1	4	19.0 ± 7.3	5	(7) 4.62	0.002 **
Spathe angle SA (°)	71.1 ± 6.3	4	42.7 ± 8.0	6	(8) 5.95	0.001***
Papilla basal area MS (μm^2)	1286 ± 378		687 ± 230			
Papilla basal area LS (μm^2)	ab		764 ± 251			

Results of independent samples *t*-test.

PA = pistillate anthesis, SA = staminate anthesis, MS = mid spathe, LS = lower spathe, ab = absent.

the stigmatic secretions of *T. wilbertii* are consumed by dipteran pollinators once trapped in the chamber is unknown – stigmatic secretions are not necessarily consumed by fly pollinators in other brood-site-mimicking arums (e.g. *A. maculatum*; Lack and Diaz 1991). Such secretions may assist with extending pollinator survival in the floral chamber, pollen adherence to insects upon egress and pollen germination (Koach, 1985 in Gibernau *et al.*, 2004; Lack and Diaz 1991).

Conserved floral traits in beetle- and fly-pollinated brood-site mimics

Floral trait diversification is largely thought to reflect variation in pollinator-mediated selection pressures (i.e. variation in their behaviour, learned preferences and innate pre-existing receiver biases) as predicted by the Grant–Stebbins model of pollinator-driven floral divergence (Grant and Grant, 1965; Stebbins, 1970; Fenster *et al.*, 2004; Johnson, 2010). Multiple traits likely to be involved in pollinator signalling were conserved between these *Typhonium* species, indicating that these traits are either similarly important for the attraction of both pollinator groups or are under diffuse selection. The colour of the inner spathe (the most prominent feature of the floral display) of *T. angustilobum* and *T. wilbertii* was comparable (Supplementary data Fig. S3), which indicated that colour was likely to be negligible in mediating differences in the pollinator attraction and capture, and that each pollinator group (associated with similar habits, i.e. decomposing substrates) may utilize similar visual stimuli, namely dark colours, to locate rewarding substrates (Chen *et al.*, 2015). A shift in pollinator assemblage was also not associated with a change in anthesis rhythms and the timing, extent and pattern of floral thermogenesis, which can vary markedly between thermogenic plant species including congeneric species (Gibernau and Barabe, 2000; Urru *et al.*, 2010; Sayers, 2019). As found in most thermogenic species (Seymour *et al.*, 2003*a*), appendix temperature increases in both species were transient and associated with enhanced insect attraction and scent emission related to a circadian rhythm.

The molecular basis of many floral traits important for pollinator attraction is largely unknown, including thermogenesis (Onda *et al.*, 2015). In this study, the appendices of both species contained two highly homologous *AOX* genes (*AOX1a* and *AOX1b*), and in both species significantly higher *AOX* transcript expression in the thermogenic appendices and thermogenic stage (unlike *pUCP*) indicated that the AOX pathway is the likely mechanism of heating, extending the range of thermogenic species in which the AOX has been identified as the major heating mechanism, including all Areae investigated to date (*Arum concinnatum*, *A. maculatum*, *Dracunculus vulgaris* and *Sauromatum guttatum*), and thermoregulatory species *Thaumatophyllum bipinnatifidum* (syn. *Philodendron bipinnatifidum*) and *Symplocarpus renifolius* (combined with UCP), both Araceae, and the eudicot *Nelumbo nucifera* (Rhoads and McIntosh, 1992; Ito and Seymour, 2005; Grant *et al.*, 2008; Onda *et al.*, 2008, 2015; Wagner *et al.*, 2008; Ito *et al.*, 2011; Miller *et al.*, 2011). Multiple *AOX* genes have similarly been identified in other thermogenic species (e.g. *A. maculatum*, *Cycas revoluta* and *N. nucifera*), in which only one *AOX* gene is likely to be the primary mediator of plant thermogenesis (Grant *et al.*, 2009; Ito *et al.*, 2011; Ito-Inaba *et al.*, 2019). Here, *AOX1b* transcripts were more highly expressed in the thermogenic appendix for both *Typhonium*

acids. Inverted triangles indicate two conserved cysteine residues (CysI and CysII). Sequences are in four groups – ENV/KNV-type, those with Ser in place of CysI (green highlight), QD/NT/S-type, and QDC-type.(*AOXs known to be activated by pyruvate; #AOXs known to be insensitive to pyruvate; ^AOXs activated by succinate). Data sources and abbreviations: AmAOX1a, 1b, 1e, 1g (*Arum maculatum* AOX1a, 1b, 1e, 1g; AB565465, BAJ22109, BAJ22112, BAJ78238); AcoAOX1a, 1b (*A. concinnatum* AOX1a, 1b; AB485993, AB485994); SrAOX1 (*Symplocarpus renifolius*; BAD83866); TaAOX1a, 1b (*T. angustilobum* AOX1a, 1b); TwAOX1a, 1b (*T. wilbertii* AOX1a, 1b), PbAOX (*Thaumatophyllum bipinnatifidum* (syn. *Philodendron bipinnatifidum*) AOX; BAD51467); NnAOX1a, 1b (*Nelumbo nucifera* AOX1a & AOX1b; AB491175 & AB491176); CrAOX1 (*Cycas revoluta*; LC081345); DvAOX (*Dracunculus vulgaris* AOX; BAD51465); SvAOX1 (*Sauromatum venosum* AOX1; P22185).

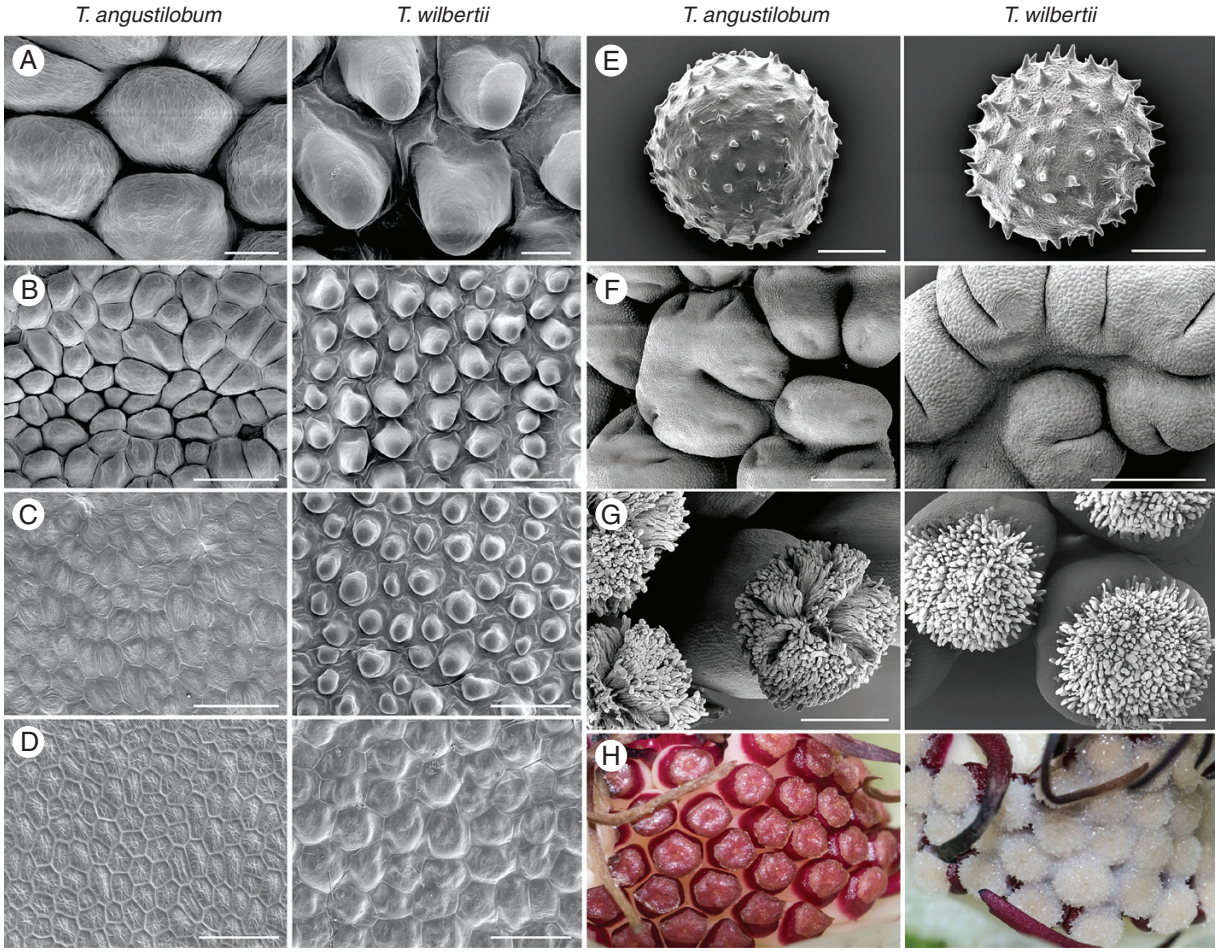

FIG. 7. SEM images: papillae on the (A, B) central and (C) lower inner spathe epidermis (1 cm above the constriction); (D) cells of the upper floral chamber epidermis; (E) pollen grains; (F) swollen pollen sacks during pistillate anthesis; (G) receptive non-thermogenic female florets. (H) Macro images of the female florets during the staminate phase of anthesis; note the stigmatic fluid produced by *T. wilbertii* (scale bars: A = 20 µm; B, C, D = 100 µm; E = 10 µm; F, G = 500 µm).

species (Fig. 6). *AOX1a* and *AOX1b* transcript expression patterns in *Typhonium* species were not consistent with the hypothesis that pyruvate-sensitive ENV-type AOX1bs may play a role in thermoregulatory species, but not in species which show transient and less controlled increases in temperature, such as *Typhonium* (Ito *et al.*, 2011).

Thermogenesis, requiring the expression of higher levels of the ubiquitous AOX (or pUCPs), has evolved independently several times in oviposition, mimicking Araceae in association with beetle and/or fly pollination (Schiestl, 2017). Increased temperature can indicate an appropriate oviposition substrate since decomposing substrates (dung, carrion or plant material) heat up due to the activity of micro-organisms (Angioy *et al.*, 2004). For example, temperature increases in the blowfly-pollinated carrion mimic *Helicodiceros muscivorus* (approx. 12 °C above ambient) are similar to those of the model substrate (gull carcass) for that species (Angioy *et al.*, 2004). However, the relationship between floral temperature increases, model substrates and specificity of thermal cues for dung-seeking pollinators remains unclear. That *T. wilbertii* thermogenic traits (heats up on average 11.4 °C to a mean peak of 38.7 °C) are more similar to those of beetle-pollinated *T. angustilobum* and *T. brownii* taxa than *T. eliosurum* (heats up on average 3.6 °C to a mean peak of 22 °C; Sayers *et al.*, 2020), which shares similar fly pollinators, raises questions about the adaptive significance of the extent of thermogenic activity and the relative importance of different sensory signals (e.g. heat and scent) for particular insect pollinators. Thermogeny alone failed to illicit a significant attractive response in dipteran pollinators of an *Arum* brood-site mimic (Kite *et al.*, 1998), and plant species visited or pollinated by Staphylinidae, for example, are not always thermogenic (Willson and Hennon, 1997; Sayers *et al.*, 2019). In addition, not all oviposition-site mimics (i.e. dung and carrion) are thermogenic (Jürgens *et al.*, 2006; Jürgens and Shuttleworth, 2015; Johnson *et al.*, 2020), although to date few non-thermogenic oviposition mimics have been reported in the Araceae (e.g. Sayers *et al.*, 2019).

Limited study of the innate responses of the saprophagous beetles and flies to thermal signals and cues, particularly in the context of oviposition sites, makes it difficult to explain the function and selection of floral thermogenic traits in pollination systems (Schiestl, 2017). From an evolutionary standpoint, two hypothesized functions for thermogenesis are proposed to account for its association with specific pollinating taxa (Schiestl, 2017). These are heating as a reward and stimuli for insects (Seymour *et al.*, 2003*b*), and/or

TABLE 4. *Mean percentage of tentative volatile compounds emitted by* T. angustilobum *and* T. wilbertii *during the pistillate phase of anthesis*

Tentative VOC identification		*T. angustilobum*			*T. wilbertii*		
		n = 12			*n* = 10		
	RI	Mean	± s.e.	O	Mean	± s.e.	O
Aliphatics							
Tetradecane‡	1400	**1.09**	**0.2**	**12**	–	–	–
Pentadecane‡	1500	**6.92**	**1.5**	**12**	**15.61**	**2.1**	**10**
2-undecanone†	1606	–	–	–	0.81	0.1	10
Methyl 4-decenoate†	1631	–	–	–	0.67	0.1	9
8-Heptadecene†	1721	–	–	–	**1.42**	**0.4**	**10**
2-Tridecanone†	1817	–	–	–	0.96	0.1	10
2-Tetradecanone†	1888	–	–	–	0.70	0.2	7
2-Pentadecanone†	2028	0.04	0.0	7	**2.49**	**0.4**	**10**
Benzenoids and phenyl propanoids							
***p*-Cresol**‡	2087	0.07	0.0	9	**2.80**	**0.4**	**10**
Nitrogen containing compounds							
Indole‡	2445	–	–	–	0.19	0.2	2
Skatole‡	2493	0.06	0.0	6	**23.52**	**2.6**	**10**
Irregular terpenes							
Neryl acetone†	1836	–	–	–	0.64	0.2	6
Dihydro-β-ionone‡	1842	–	–	–	**5.29**	**1.6**	**10**
α-Ionone†	1862	–	–	–	**1.68**	**0.3**	**10**
β-Ionone‡	1950	–	–	–	**6.42**	**0.9**	**10**
Sesquiterpenes							
δ-Elemene†	1465	**1.12**	**0.0**	**12**	–	–	–
Elemene isomer†	1493	**12.35**	**0.5**	**12**	–	–	–
α-Copaene‡	1495	0.13	0.0	12	0.67	0.5	2
β-Maaliene†	1548	0.46	0.1	11	–	–	–
Aristolene†	1573	**1.65**	**0.2**	**12**	–	–	–
(2*Z*,4*E*)-3,7,11-trimethyl-2,4-dodecadiene*	1590	–	–	–	**5.44**	**1.4**	**10**
β-Elemene†	1597	**4.85**	**0.4**	**12**	–	–	–
β-Gurjunene†	1600	**7.05**	**0.9**	**12**	–	–	–
β-Caryophyllene‡	1603	**0.97**	**0.3**	**11**	1.39	0.9	2
α-Maaliene†	1607	**0.97**	**0.1**	**12**	–	–	–
Aromadendrene†	1613	0.73	0.1	12	–	–	–
Selina-5,11-diene†	1620	0.46	0.0	12	–	–	–
Allo-aromadendrene†	1651	0.39	0.0	12	0.32	0.2	2
α-Humulene‡	1677	0.66	0.1	12	2.09	1.4	2
γ-Muurolene†	1694	0.32	0.0	12	0.29	0.2	2
Capparatriene†	1700	–	–	–	**11.37**	**1.7**	**10**
Viridiflorene†	1705	**1.18**	**0.1**	**12**	–	–	–
Germacrene D†	1716	–	–	–	0.29	0.2	2
β-Selinene†	1727	0.17	0.1	3¶	0.43	0.2	4
α-Selinene†	1731	0.16	0.1	3¶	0.65	0.3	4
Bicyclogermacrene†	1741	**53.18**	**1.9**	**12**	0.30	0.1	4
δ-Cadinene†	1763	0.41	0.1	12	1.14	0.8	2
Selina-3,7(11)-diene†	1786	0.52	0.1	12	1.35	0.7	3
Spathulenol†	2130	0.55	0.1	12	–	–	–
Isospathulenol†	2230	0.09	0.0	12	–	–	–
Major unknowns							
Unknown *m/z* 69, 81, 41, 95, 67, 55	1534	**1.37**	**0.3**	**12**	–	–	–
Unknown *m/z* 204, 189, 105, 161, 91, 147	1630	**0.98**	**0.1**	**12**	–	–	–
Unknown *m/z* 58, 43, 71, 41, 59, 55	1677	–	–	–	**4.03**	**1.2**	**8**
Unknown *m/z* 70, 55, 69, 83, 97, 57	2236	–	–	–	**2.29**	**0.5**	**9**
Unknown *m/z* 83, 55, 69, 97,43, 57	2371	0.06	0.0	7	**1.87**	**0.6**	**10**
Minor pooled unknowns (peak area < 1.0 %)§		1.07 [7]			2.87 [5]		

VOCs with mean peak areas >1 % that occurred in the majority of samples are highlighted in bold, *n* = number of replicates.

RI = retention index, O = number of chromatograms where VOC was recorded.

– Indicates absence of the compound in sample chromatograms, or compound below the threshold of integration or detection.

*>95 % compound match with NIST14.

†Identification supported by RI.

‡Identification confirmed by authentic standard.

§Minor unknowns were pooled, with the superscript digit providing the number of pooled compounds.

¶Compound peaks could not be resolved in some chromatograms due to interference with neighbouring compounds.

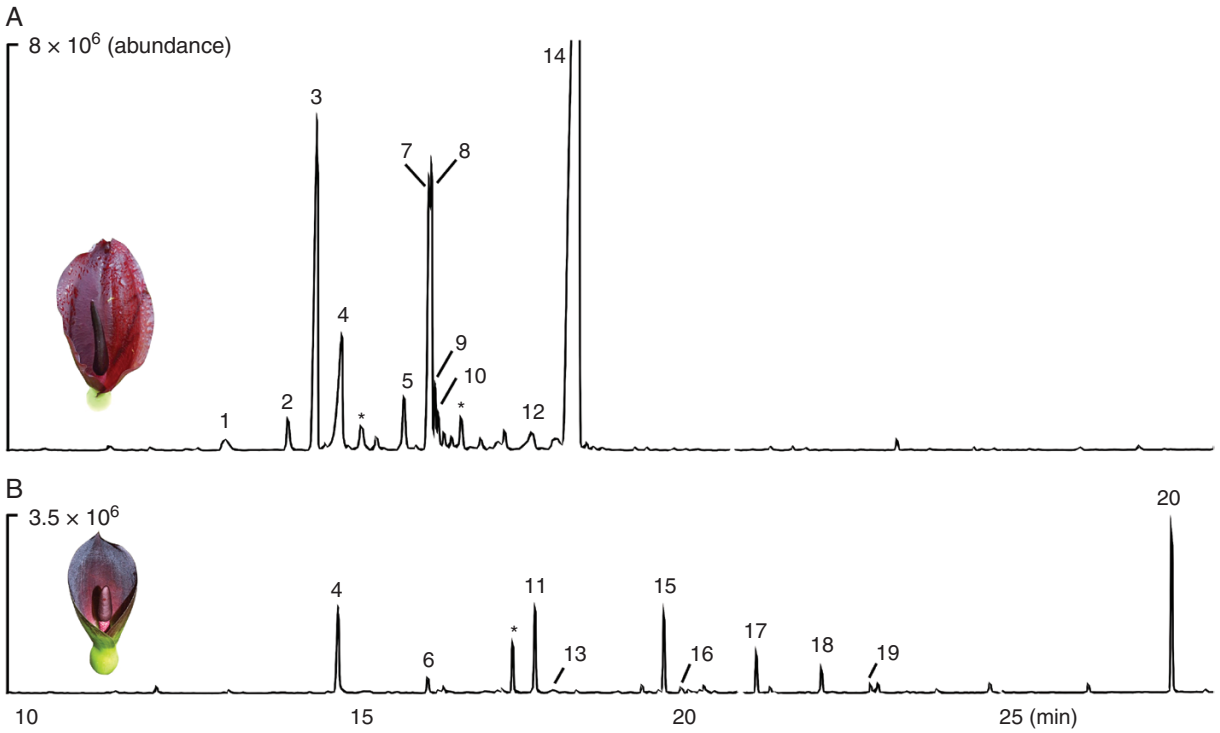

FIG. 8. Typical gas chromatograms of (A) *T. angustilobum* and (B) *T. wilbertii*, the major floral compounds identified (which account most for high levels of similarity within species according to SIMPER analyses) include: (1) tetradecane, (2) δ-elemene, (3) elemene isomer, (4) pentadecane, (5) aristolene, (6) (2*Z*,4*E*)-3,7,11-trimethyl-2,4-dodecadiene, (7) β-elemene, (8) β-gurjunene, (9) β-caryophyllene, (10) α-maaliene, (11) capparatriene, (12) viridiflorene, (13) 8-heptadecene, (14) bicyclogermacrene, (15) dihydro-β-ionone, (16) α-ionone, (17) β-ionone, (18) 2-pentadecanone, (19) *p*-cresol and (20) skatole (*major unknown compounds).

heating as a deceptive signal for pollinators to associate with a rewarding substrate (i.e. decomposing material) in brood-site mimics through exploiting the pre-existing bias of pollinators (Schiestl, 2017). Only Angioy *et al.* (2004) provide evidence for thermogenesis as a direct pollinator (blowfly) lure, in combination with scent, in *H. muscivorus*. Based on our results, we similarly suggest that heating as a direct signal for saprophagous beetles and flies explains the occurrence of thermogenesis (an energetically expensive process) in these two rewardless brood-site mimics which may also act synergistically with scent for enhanced pollinator attraction (Angioy *et al.*, 2004; Marotz-Clausen *et al.*, 2018), particularly since, in contrast to some thermogenic Araceae (e.g. Seymour *et al.*, 2003*a*; Ito *et al.*, 2011), no thermogenic organs were present inside the floral chamber where trapped insects reside (i.e. the appendix and staminate zone are above the spathe constriction in *Typhonium*). Heating in staminate tissues throughout the night and prior to pollen shed may also assist with pollen development (Seymour *et al.*, 2009*b*). Neither the genetics, expression or profile of thermogenesis, nor the colour was associated with pollinator divergence, indicating that morphology and floral scent are likely to be more important for pollinator differentiation.

Floral trait divergence: pollinators as selective agents?

The scent profiles of *T. angustilobum* and *T. wilbertii* differed significantly. High relative amounts of the common dung constituents skatole and *p*-cresol (Dormont *et al.*, 2010; Stavert *et al.*, 2014; Frank *et al.*, 2018) in combination with sesquiterpenes and irregular terpenes emitted by *T. wilbertii* indicate that this species is a dung mimic which exploits the pre-existing sensory (olfactory) bias of diverse fly pollinators (Urru *et al.*, 2011; Jürgens and Shuttleworth, 2015). A sub-set of scent compounds may be sufficient for the attraction of dung-seeking flies to thermogenic and non-thermogenic species (Leguet *et al.*, 2014; Delle-Vedove *et al.*, 2017). For example, the emission of *p*-cresol and/or skatole is commonly associated with dung and dung mimics (e.g. Quilichini *et al.*, 2010; Urru *et al.*, 2011; Johnson *et al.*, 2020), and these are likely to be important for the attraction of saprophagous flies (e.g. Sphaeroceridae) to *T. wilbertii* as shown for fly-pollinated *T. eliosurum* (Sayers *et al.*, 2020). The VOC *p*-cresol alone, emitted by thermogenic *Arum maculatum*, was highly attractive to Psychodidae pollinators (Kite *et al.*, 1998), and in non-thermogenic *Wurmbea* the addition of skatole (and indole) to the non-faecal mimic *W. kraussii* shifted the attracted insect assemblage to one dominated by coprophagous flies (Johnson *et al.*, 2020).

Typhonium angustilobum was dominated by a complex array of sesquiterpenes, and *p*-cresol and skatole were only emitted at very low levels or were not detected at all in some inflorescences. This contrasts with the staphylinid- and scarab-pollinated *T. brownii* which consistently emitted high relative amounts of skatole and *p*-cresol, in addition to minor amounts of indole (Sayers *et al.*, 2020), the latter not detected in *T. angustilobum*. Another staphylinid pollination system showed that the emission of indole by the non-thermogenic

Lysichiton americanus (Araceae) is the primary attractant of *Pelecomalium testaceum* (Willson and Hennon, 1997; Brodie *et al.*, 2018). The lack of known staphylinid attractants in the scent profile of *T. angustilobum* and the highly varied function of terpenes in plants means that it is unclear which VOCs are important for pollinator attraction in this system (Theis and Lerdau, 2003). The role of sesquiterpenes (e.g. bicyclogermacrene) and other terpenes in the attraction of saprophagous beetles (i.e. Staphylinidae) and flies is poorly understood, despite sesquiterpenes being a common odour component of dung and floral dung mimics (Kite *et al.*, 1998; Dormont *et al.*, 2010; Chartier *et al.*, 2013). Despite these limitations, the scent profile, presence of saprophagous or predacious insects and absence of rewards suggest that *T. angustilobum* is a brood-site mimic which may mimic a substrate of a different trophic level or stage of decomposition (e.g. decomposing plant material; Jürgens and Shuttleworth, 2015).

Studies of convergent evolution of oviposition mimicry among plant taxa suggest that brood-site deception relies on olfactory stimuli as the main modality for pollinator attraction (Jürgens *et al.*, 2013). Indeed, the floral scent of brood-site mimics has been shown to be sufficient to attract pollinators in the absence of other stimuli (e.g. Kite *et al.*, 1998; Angioy *et al.*, 2004; Johnson *et al.*, 2020; Sayers *et al.*, 2020). Although several studies in Araceae show that single VOCs or simple VOC combinations can selectively attract pollinators, particularly Cyclocephaline scarab beetles (e.g. Maia *et al.*, 2012, 2013; Pereira *et al.*, 2014), overall little is known about the behavioural responses of beetles and flies to specific olfactory cues or signals (Francke and Dettner, 2005), and the extent to which these divergent *Typhonium* scents reflect adaptation to the different receiver biases of beetle and fly pollinators warrants further investigation (using bioassays and electroantennography). Although scent differentiation between *T. angustilobum* and *T. wilbertii* may reflect adaptation to divergent pollinators, we reiterate that flies (e.g. Sphaeroceridae and Sepsidae) were observed in large numbers on the spathe of *T. angustilobum* (Fig. 3B, C), and beetles (e.g. Staphylinidae) were attracted and trapped by *T. wilbertii* (albeit in lower numbers; Fig. 2), questioning the relative importance of scent in selectively attracting and (more importantly) trapping divergent pollinator assemblages in brood-site mimics (Armbruster, 2017).

Changes in morphological traits are often associated with shifts to fly pollination among phylogenetically related plant taxa in general (Fenster *et al.*, 2004), and, among fly pollinated brood-site mimics, both chemical and morphological filters have been identified to play a role in greater pollinator specialization (Shuttleworth *et al.*, 2017; Raguso, 2020). Floral traps are prevalent in the Aroideae (particularly fly-pollinated systems) in mutualistic and deceptive plant–pollinator interactions, and in some genera the spathe plays a critical role in the trapping of insect pollinators (Bröderbauer *et al.*, 2012). Spadices and spathes of beetle-pollinated *T. angustilobum* were significantly larger compared with *T. wilbertii* in which the smaller spathe was more tightly wrapped around the spadix during both reproductive phases (Fig. 5), more similar to spathe orientation in fly-pollinated *T. eliosurum* (Sayers *et al.*, 2020). Flies are typically more agile fliers than beetles, and this spathe morphology probably assists in trapping flies and ensuring contact with staminate florets as they exit the floral chamber (Fig. 4G, H). Further, while the inner spathe epidermis of both species comprised curved cells as found in other floral trap systems (Poppinga *et al.*, 2010), the cells of *T. wilbertii* were smaller, less densely packed and more refined downward pointing papillae (similar to the fly-pollinated *T. eliosurum*), distributed down the spathe blade to the floral chamber entrance, which may reduce the attachment of flies (see Sayers *et al.*, 2020). Bröderbauer *et al.* (2013) similarly identified that midge-pollinated (primarily Psychodidae) *Arum* species were characterized by smaller inner spathe papillae compared with species pollinated by both flies and beetles, or bees. They also identified differences in the number of sterile filiform organs of *Arum* species pollinated by midges or both flies and beetles (Bröderbauer *et al.*, 2013). These organs are assumed to help retain insects inside the floral chamber close to the female florets (Fig. 3D). Spadices of both *T. angustilobum* and *T. wilbertii* comprised filiform organs directly above the female florets (Fig. 1), similar to the beetle-pollinated *T. brownii* complex (Sayers *et al.*, 2020). The portion of interstice above the sterile filiform organs was naked in beetle-pollinated *T. angustilobum* and the *T. brownii* complex, but comprised some sparse, smaller papillate organs in fly-pollinated *T. wilbertii*, which were more extensive in the fly-pollinated *T. eliosurum* (Sayers *et al.*, 2020). More detailed comparison of trapping features across the genus and potential adaptation to different pollinators is merited.

Conclusions

Typhonium angustilobum and *T. wilbertii* are two closely related brood-site mimics characterized by similar dull, dark floral colours, anthesis rhythms and transient heat generation (via the AOX pathway) which probably acts synergistically with enhanced scent volatilization to attract diverse saprophagous insect pollinators. Divergent scents, apparently resembling different decomposing substrates, and differences in floral morphology and trapping mechanisms (not involved in mimicry), indicate that both chemical and morphological filters contribute to taxonomic and functional specialization to different groups of pollinating Coleoptera and Diptera by *T. angustilobum* and *T. wilbertii*, respectively. This study demonstrates the importance of comprehensive trait characterization of multisensory signals and floral morphology in understanding floral trait adaptation to different pollinator groups in brood-site mimetic systems. These pollination systems provide an interesting avenue for further research into the evolution of certain floral traits for pollinator attraction possibly associated with the receiver bias hypothesis. In particular, additional research is required to clarify if thermogenesis in brood-site mimics has developed as the result of pre-existing insect responses to the temperature cues of decomposing substrates. Overall, we suggest that the maintenance of complex beetle- or fly-attracting floral odours, and unique floral morphologies, reflects the diffuse selection imposed by the diverse and dynamic insect communities by which each species is visited across their respective geographic ranges.

SUPPLEMENTARY DATA

Supplementary data are available online at https://academic.oup.com/aob and consist of the following. Table

S1: primer information for RT–qPCR and sequencing of *T. angustilobum* and *T. wilbertii AOX* genes. Figure S1: partial protein alignment of *T. wilbertii* and *T. angustilobum* AOX1s and percentage identity matrix for AOX proteins from *T. angustilobum*, *T. wilbertii* and 12 AOXs from other thermogenic taxa. Figure S2: deduced amino acid sequences of *T. angustilobum* and *T. wilbertii* proteins aligned with those of previously reported AOXs expressed in thermogenic tissues. Figure S3: mean reflectance of the inner spathe of *T. angustilobum* and *T. wilbertii* during the pistillate phase of anthesis.

FUNDING

This work was supported by the Ecological Society of Australia and the Holsworth Wildlife Research Endowment granted to T.D.J.S., and the Hermon Slade Foundation (HSF09/07) granted to R.E.M. whose lectureship received support from the Cybec Foundation. GC-MS equipment was part funded by an Australian Research Council grant FT100100199 to M.J.S.

ACKNOWLEDGEMENTS

We thank Bruce Gray, David Baume and the Roberts family (Charlie, Lewis and Edith) for providing study material and information on field locations in Far North Queensland. Thanks also to our field assistant Odette Simpson (funded by M.J.S.); Margaret Thayer (Field Museum of Natural History, Chicago) for the identification of Staphylinidae and Hydrophilidae; the Insect–Plant Interactions Lab (La Trobe University) for use of GC-MS; the University of Melbourne Biosciences Microscopy Unit (BMU-05); Amanpreet Gaur (La Trobe University) for technical lab assistance; and Jennifer Fox (University of Melbourne) for initial primer design. Research was undertaken with the support of the QLD Department of Environment and Heritage Protection under permit number WITK162116315. T.D.J.S. and R.E.M. conceived and designed the study with input from K.L.J., M.J.S. and K.F. T.D.J.S. and R.E.M. collected and analysed the field data, K.L.J. assisted with molecular analyses, and K.F. and M.J.S. assisted with scent analyses. GC-MS equipment was provided by M.J.S. All authors contributed critically to the manuscript drafts and gave final approval for publication.

LITERATURE CITED

Albre J, Quilichini A, Gibernau M. 2003. Pollination ecology of *Arum italicum* (Araceae). *Botanical Journal of the Linnean Society* **141**: 205–214.

Angioy AM, Stensmyr MC, Urru I, Puliafito M, Collu I, Hansson BS. 2004. Function of the heater: the dead horse arum revisited. *Proceedings of the Royal Society B: Biological Sciences* **271**(Suppl 3): S13–S15.

Armbruster WS. 2017. The specialization continuum in pollination systems: diversity of concepts and implications for ecology, evolution and conservation. *Functional Ecology* **31**: 88–100.

Arriaga-Varela E, Wong SY, Kirejtshuk A, Fikáček M. 2018. Review of the flower-inhabiting water scavenger beetle genus *Cycreon* (Coleoptera, Hydrophilidae), with descriptions of new species and comments on its biology. *Deutsche Entomologische Zeitschrift* **65**: 99–115.

Banerji I. 1947. Life history of *Typhonium trilobatum* Schott. *Proceedings of the National Institute of Sciences, India* **13**: 207–230.

Berthold DA, Andersson ME, Nordlund P. 2000. New insight into the structure and function of the alternative oxidase. *Biochimica et Biophysica Acta* **1460**: 241–254.

Bishop AL, McKenzie HJ, Barchia IM, Harris AM. 1998. Occurrence and effect of temperature regimes on four species of fly (Diptera) found with *Culicoides brevitarsis* Kieffer (Ceratopogonidae) in bovine dung. *Journal of the Entomological Society of New South Wales* **28**: 93–99.

Borecký J, Vercesi AE. 2005. Plant uncoupling mitochondrial protein and alternative oxidase: energy metabolism and stress. *Bioscience Reports* **25**: 271–286.

Boyce PC, Croat TB. 2018. The Überlist of Araceae, totals for published and estimated number of species in aroid genera. http://www.aroid.org/genera/180211uberlist.pdf, accessed 14 February 2021.

Bröderbauer D, Diaz A, Weber A. 2012. Reconstructing the origin and elaboration of insect-trapping inflorescences in the Araceae. *American Journal of Botany* **99**: 1666–1679.

Bröderbauer D, Weber A, Diaz A. 2013. The design of trapping devices in pollination traps of the genus Arum (Araceae) is related to insect type. *Botanical Journal of the Linnean Society* **172**: 385–397.

Brodie BS, Renyard A, Gries R, *et al.* 2018. Identification and field testing of floral odorants that attract the rove beetle *Pelecomalium testaceum* (Mannerheim) to skunk cabbage, *Lysichiton americanus* (L.). *Arthropod-Plant Interactions* **12**: 591–599.

Burton RA, Shirley NJ, King BJ, Harvey AJ, Fincher GB. 2004. The CesA gene family of barley. Quantitative analysis of transcripts reveals two groups of co-expressed genes. *Plant Physiology* **134**: 224–236.

Burton RA, Jobling SA, Harvey AJ, *et al.* 2008. The genetics and transcriptional profiles of the cellulose synthase-like HvCslF gene family in barley. *Plant Physiology* **146**: 1821–1833.

Bustin SA. 2000. Absolute quantification of mRNA using real-time reverse transcription polymerase chain reaction assays. *Journal of Molecular Endocrinology* **25**: 169–193.

Campbell MM. 1976. Periodicity of four Diptera and one Coleoptera on fresh cow dung in south-east Queensland. *Journal of Natural History* **10**: 601–606.

Chartier M, Pélozuelo L, Buatois B, Bessière J-M, Gibernau M, Ayasse M. 2013. Geographical variations of odour and pollinators, and test for local adaptation by reciprocal transplant of two European *Arum* species. *Functional Ecology* **27**: 1367–1381.

Chartier M, Gibernau M, Renner SS. 2014. The evolution of pollinator–plant interaction types in the Araceae. *Evolution* **68**: 1533–1543.

Chen G, Ma XK, Jürgens A, *et al.* 2015. Mimicking livor mortis: a well-known but unsubstantiated color profile in sapromyiophily. *Journal of Chemical Ecology* **41**: 808–815.

Clarke KR, Gorley RN. 2015. *PRIMER v7: User Manual/Tutorial*. Ivybridge, UK. PRIMER-E Ltd.

Cleghorn ML. 1914. A note on the floral mechanism of *Typhonium trilobatum*. *Journal of the Proceedings of the Asiatic Society of Bengal* **10**: 421–424.

Crichton PG, Affourtit C, Albury MS, Carré JE, Moore AL. 2005. Constitutive activity of *Sauromatum guttatum* alternative oxidase in *Schizosaccharomyces pombe* implicates residues in addition to conserved cysteines in alpha-keto acid activation. *FEBS Letters* **579**: 331–336.

Cusimano N, Barrett MD, Hetterscheid WLA, Renner SS. 2010. A phylogeny of the Areae (Araceae) implies that *Typhonium*, *Sauromatum*, and the Australian species of *Typhonium* are distinct clades. *International Association for Plant Taxonomy* **59**: 439–447.

Dafni A. 1984. Mimicry and deception in pollination. *Annual Review of Ecology and Systematics* **15**: 259–278.

Davis ALV. 1994. Associations of Afrotropical Coleoptera (Scarabaeidae: Aphodiidae: Staphylinidae: Hydrophilidae: Histeridae) with dung and decaying matter: implications for selection of fly-control agents for Australia. *Journal of Natural History* **28**: 383–399.

Delle-Vedove R, Schatz B, Dufay M. 2017. Understanding intraspecific variation of floral scent in light of evolutionary ecology. *Annals of Botany* **120**: 1–20.

Dormont L, Jay-Robert P, Bessière JM, Rapior S, Lumaret JP. 2010. Innate olfactory preferences in dung beetles. *Journal of Experimental Biology* **213**: 3177–3186.

Fenster CB, Armbruster WS, Wilson P, Dudash MR, Thomson JD. 2004. Pollination syndromes and floral specialization. *Annual Review of Ecology, Evolution, and Systematics* **35**: 375–403.

Francke W, Dettner K. 2005. Chemical signalling in beetles. *Topics in Current Chemistry* **240**: 85–166.

Frank K, Brüchner A, Blüthgen N, Schmitt T. 2018. In search of cues: dung beetle attraction and the significance of volatile composition of dung. *Chemoecology* **28**: 145–152.

Gibernau M. 2011. Pollinators and visitors of aroid inflorescences: an addendum. *Aroideana* **34**: 70–83.

Gibernau M, Barabe D. 2000. Thermogenesis in three *Philodendron* species (Araceae) of French Guiana. *Canadian Journal of Botany* **78**: 685–689.

Gibernau M, Macquart D, Przetak G. 2004. Pollination in the genus *Arum* – a review. *Aroideana*, **27**: 148–166.

Gibernau M, Chartier M, Barabé D. 2010. Recent advances towards an evolutionary comprehension of Araceae pollination. In: Seberg O, Petersen G, Barfod AS, Davis JI, eds. *Diversity, phylogeny, and evolution in the Monocotyledons*. Denmark: Aarhus University Press, 101–114.

Grant NM, Miller RE, Watling JR, Robinson SA. 2008. Synchronicity of thermogenic activity, alternative pathway respiratory flux, AOX protein content, and carbohydrates in receptacle tissues of sacred lotus during floral development. *Journal of Experimental Botany* **59**: 705–714.

Grant N, Onda Y, Kakizaki Y, Ito K, Watling J, Robinson S. 2009. Two cys or not two cys? That is the question; alternative oxidase in the thermogenic plant sacred Lotus. *Plant Physiology* **150**: 987–995.

Grant V, Grant KA. 1965. *Flower pollination in the phlox family*. New York: Columbia University Press.

Hay A. 2011. Araceae. In: Wilson A, ed. *Flora of Australia. Volume 39. Alismatales to Arales*. Canberra: CSIRO Publishing, 236–274.

Hoe YC, Gibernau M, Wong SY. 2018. Diversity of pollination ecology in the *Schismatoglottis calyptrata* Complex clade (Araceae). *Plant Biology (Stuttgart, Germany)* **20**: 563–578.

Hu GY, Frank JH. 1997. Predation on the horn fly (Diptera: Muscidae) by five species of *Philonthus* (Coleoptera: Staphylinidae). *Environmental Entomology* **26**: 1240–1246.

Ito K, Seymour RS. 2005. Expression of uncoupling protein and alternative oxidase depends on lipid or carbohydrate substrates in thermogenic plants. *Biology Letters* **1**: 427–430.

Ito K, Ogata T, Kakizaki Y, Elliott C, Albury MS, Moore AL. 2011. Identification of a gene for pyruvate-insensitive mitochondrial alternative oxidase expressed in the thermogenic appendices in *Arum maculatum*. *Plant Physiology* **157**: 1721–1732.

Ito-Inaba Y, Hida Y, Ichikawa M, Kato Y, Yamashita T. 2008. Characterization of the plant uncoupling protein, SrUCPA, expressed in spadix mitochondria of the thermogenic skunk cabbage. *Journal of Experimental Botany* **59**: 995–1005.

Ito-Inaba Y, Sato M, Sato MP, *et al.* 2019. Alternative oxidase capacity of mitochondria in microsporophylls may function in cycad thermogenesis. *Plant Physiology* **180**: 743–756.

Johnson SD. 2010. The pollination niche and its role in the diversification and maintenance of the southern African flora. *Philosophical Transactions of the Royal Society B: Biological Sciences* **365**: 499–516.

Johnson SD, Schiestl FP. 2016. *Floral mimicry*. Oxford: Oxford University Press.

Johnson SD, Sivechurran J, Doarsamy S, Shuttleworth A. 2020. Dung mimicry: the function of volatile emissions and corolla patterning in fly-pollinated Wurmbea flowers. *New Phytologist* **228**: 1662–1673.

Jürgens A, Shuttleworth A. 2015. Carrion and dung mimicry in plants. In: Benbow ME, Tomberlin JK, Tarone AM, eds. *Carrion ecology, evolution, and their applications*. Boca Raton, FL: CRC Press, 361–386.

Jürgens A, Dötterl S, Ulrich M. 2006. The chemical nature of fetid floral odours in stapeliads (Apocynaceae-Asclepiadoideae-Ceropegieae). *New Phytologist* **172**: 452–468.

Jürgens A, Wee SL, Shuttleworth A, Johnson SD. 2013. Chemical mimicry of insect oviposition sites: a global analysis of convergence in angiosperms. *Ecology Letters* **16**: 1157–1167.

Kite GC, Hetterscheid WLA. 2017. Phylogenetic trends in the evolution of inflorescence odours in Amorphophallus. *Phytochemistry* **142**: 126–142.

Kite GC, Hetterscheid WLA, Lewis ML, *et al.* 1998. Inflorescence odours and pollinators of *Arum* and *Amorphophallus* (Araceae). In: Owens SJ, Rudall PJ, eds. *Reproductive biology*. Kew: Royal Botanic Gardens, 295–315.

Knudsen JT, Eriksson R, Gershenzon J, Stahl B. 2006. Diversity and distribution of floral scent. *Botanical Review* **72**: 1–120.

Koach, J. 1985. *Bio-ecological studies of flowering and pollination in Israeli Araceae*. PhD Dissertation, University of Tel-Aviv, Israel.

van der Kooi CJ, Ollerton J. 2020. The origins of flowering plants and pollinators. *Science* **368**: 1306–1308.

Lack AJ, Diaz A. 1991. Pollination of *Arum maculatum* L. – a historical review and new observations. *Watsonia* **18**: 333–342.

Lawrence JF, Ślipiński A. 2013. *Australian beetles. Volume 1: morphology, classification and keys*. Collingwood: CSIRO Publishing.

Leguet A, Gibernau M, Shintu L, *et al.* 2014. Evidence for early intracellular accumulation of volatile compounds during spadix development in *Arum italicum* L. and preliminary data on some tropical Aroids. *Die Naturwissenschaften* **101**: 623–635.

Li JK, Huang SQ. 2009. Flower thermoregulation facilitates fertilization in Asian sacred lotus. *Annals of Botany* **103**: 1159–1163.

Maia ACD, Dötterl S, Kaiser R, *et al.* 2012. The key role of 4-methyl-5-vinylthiazole in the attraction of scarab beetle pollinators: a unique olfactory floral signal shared by Annonaceae and Araceae. *Journal of Chemical Ecology* **38**: 1072–1080.

Maia AC, Gibernau M, Dötterl S, *et al.* 2013. The floral scent of *Taccarum ulei* (Araceae): attraction of scarab beetle pollinators to an unusual aliphatic acyloin. *Phytochemistry* **93**: 71–78.

Marotz-Clausen G, Jürschik S, Fuchs R, *et al.* 2018. Incomplete synchrony of inflorescence scent and temperature patterns in *Arum maculatum* L. (Araceae). *Phytochemistry* **154**: 77–84.

Mayo SJ, Bogner J, Boyce PC. 1997. *The genera of Araceae*. Kew: Royal Botanic Gardens.

McKenna DD, Shin S, Ahrens D, *et al.* 2019. The evolution and genomic basis of beetle diversity. *Proceedings of the National Academy of Sciences, USA* **116**: 24729–24737.

Meeuse BJD, Raskin I. 1988. Sexual reproduction in the arum lily family, with emphasis on thermogenicity. *Sexual Plant Reproduction* **1**: 3–15.

Miller RE, Grant NM, Giles L, *et al.* 2011. In the heat of the night – alternative pathway respiration drives thermogenesis in *Philodendron bipinnatifidum*. *New Phytologist* **189**: 1013–1026.

Moretto P, Cosson B, Krell FT, Aristophanous M. 2019. Pollination of *Amorphophallus barthlottii* and *A. abyssinicus* subsp. *akeassii* (Araceae) by dung beetles (Insecta: Coleoptera: Scarabaeoidea). *Catharsius La Revue* **18**: 19–36.

Nauheimer L, Metzler D, Renner SS. 2012. Global history of the ancient monocot family Araceae inferred with models accounting for past continental positions and previous ranges based on fossils. *New Phytologist* **195**: 938–950.

Ollerton J, Winfree R, Tarrant S. 2011. How many flowering plants are pollinated by animals? *Oikos* **120**: 321–326.

Onda Y, Kato Y, Abe Y, *et al.* 2007. Pyruvate-sensitive AOX exists as a non-covalently associated dimer in the homeothermic spadix of the skunk cabbage, *Symplocarpus renifolius*. *FEBS Letters* **581**: 5852–5858.

Onda Y, Kato Y, Abe Y, *et al.* 2008. Functional coexpression of the mitochondrial alternative oxidase and uncoupling protein underlies thermoregulation in the thermogenic florets of skunk cabbage. *Plant Physiology* **146**: 636–645.

Onda Y, Mochida K, Yoshida T, *et al.* 2015. Transcriptome analysis of thermogenic *Arum concinnatum* reveals the molecular components of floral scent production. *Scientific Reports* **5**: 8753.

Pellmyr O, Patt JM. 1986. Function of olfactory and visual stimuli in pollination of *Lysichiton americanum* (Araceae) by a staphylinid beetle. *Madroño* **33**: 47–54.

Pereira J, Schlindwein C, Antonini Y, *et al.* 2014. *Philodendron adamantinum* (Araceae) lures its single cyclocephaline scarab pollinator with specific dominant floral scent volatiles. *Biological Journal of the Linnean Society* **111**: 679–691.

Poppinga S, Koch K, Bohn HF, Barthlott W. 2010. Comparative and functional morphology of hierarchically structured anti-adhesive surfaces in carnivorous plants and kettle trap flowers. *Functional Plant Biology* **37**: 952–961.

Quilichini A, Macquart D, Barabé D, Albre J, Gibernau M. 2010. Reproduction of the West Mediterranean endemic *Arum pictum* (Araceae) on Corsica. *Plant Systematics and Evolution* **287**: 179–187.

Raguso RA. 2020. Don't forget the flies: dipteran diversity and its consequences for floral ecology and evolution. *Applied Entomology and Zoology* **55**: 1–7.

Renner SS. 2006. Rewardless flowers in the angiosperms and the role of insect cognition in their evolution. In: Waser NM, Ollerton J, eds. *Plant–pollinator interactions: from specialization to generalization.* Chicago, IL: University of Chicago, 123–144.

Rhoads DM, McIntosh L. 1992. Salicylic acid regulation of respiration in higher plants: alternative oxidase expression. *The Plant Cell* **4**: 1131–1139.

Sayers TDJ. 2019. *The ecology and evolution of plant-pollinator interactions in Australian Typhonium (Araceae)*. PhD Dissertation, The University of Melbourne.

Sayers TDJ, Steinbauer MJ, Miller RE. 2019. Visitor or vector? The extent of rove beetle (Coleoptera: Staphylinidae) pollination and floral interactions. *Arthropod-Plant Interactions* **13**: 685–701.

Sayers TDJ, Steinbauer MJ, Farnier K, Miller RE. 2020. Dung mimicry in *Typhonium* (Araceae): explaining floral trait and pollinator divergence in a widespread species complex and rare sister species. *Botanical Journal of the Linnean Society* **193**: 375–401.

Schaefer HM, Ruxton GD. 2011. *Plant–animal communication*. Oxford: Oxford University Press.

Schiestl FP. 2017. Innate receiver bias: its role in the ecology and evolution of plant–animal interactions. *Annual Review of Ecology, Evolution, and Systematics* **48**: 585–603.

Schiestl FP, Dötterl S. 2012. The evolution of floral scent and olfactory preferences in pollinators: coevolution or pre-existing bias? *Evolution* **66**: 2042–2055.

Schiestl FP, Johnson SD. 2013. Pollinator-mediated evolution of floral signals. *Trends in Ecology & Evolution* **28**: 307–315.

Seymour RS, Matthews PG. 2006. The role of thermogenesis in the pollination biology of the Amazon waterlily *Victoria amazonica*. *Annals of Botany* **98**: 1129–1135.

Seymour RS, Schultze-Motel P. 1997. Heat-producing flowers. *Endeavour* **21**: 125–129.

Seymour RS, Gibernau M, Ito K. 2003*a*. Thermogenesis and respiration of inflorescences of the dead horse arum *Helicodiceros muscivorus*, a pseudo-thermoregulatory aroid associated with fly pollination. *Functional Ecology* **17**: 886–894.

Seymour RS, White CR, Gibernau M. 2003*b*. Environmental biology: heat reward for insect pollinators. *Nature* **426**: 243–244.

Seymour RS, Gibernau M, Pirintsos SA. 2009*a*. Thermogenesis of three species of Arum from Crete. *Plant, Cell & Environment* **32**: 1467–1476.

Seymour RS, Ito Y, Onda Y, Ito K. 2009*b*. Effects of floral thermogenesis on pollen function in Asian skunk cabbage *Symplocarpus renifolius*. *Biology Letters* **5**: 568–570.

Shuttleworth A, Johnson SD, Jürgens A. 2017. Entering through the narrow gate: a morphological filter explains specialized pollination of a carrion-scented stapeliad. *Flora* **232**: 92–103.

Sivadasan M, Kavalan R. 2005. Flowering phenology and beetle pollination in *Theriophonum infaustum* N.E.Br. (Araceae). *Aroideana* **28**: 104–112.

Stavert JR, Drayton BA, Beggs JR, Gaskett AC. 2014. The volatile organic compounds of introduced and native dung and carrion and their role in dung beetle foraging behaviour. *Ecological Entomology* **39**: 556–565.

Stavert JR, Liñán-Cembrano G, Beggs JR, Howlett BG, Pattemore DE, Bartomeus I. 2016. Hairiness: the missing link between pollinators and pollination. *Peerj* **4**: e2779.

Stebbins GL. 1970. Adaptive radiation of reproductive characteristics in angiosperms, 1: pollination mechanisms. *Annual Review of Ecology and Systematics* **1**: 307–326.

Stebnicka ZT, Howden HF. 1995. Revision of Australian genera in the tribes Aphodiini, Aegialiini and Proctophanini (Coleoptera: Scarabaeidae: Aphodiinae). *Invertebrate Taxonomy* **9**: 709–766.

Thayer MK. 2016. 14.7 Staphylinidae Latreille, 1802. In: Beutel RG, Leschen RAB, eds. *Handbook of Zoology, Arthropoda: Insecta; Coleoptera, beetles. Morphology and systematics (Archostemata, Adephaga, Myxophaga, Polyphaga partim)*, 2nd edn. Berlin, Boston: De Gruyter, 394–442.

Theis N, Lerdau M. 2003. The evolution of function in plant secondary metabolites. *International Journal of Plant Sciences* **164**: S93–S102.

Tholl D, Boland W, Hansel A, Loreto F, Röse US, Schnitzler JP. 2006. Practical approaches to plant volatile analysis. *The Plant Journal* **45**: 540–560.

Thompson JN. 1994. *The coevolutionary process*. Chicago: University of Chicago Press.

Urru I, Stökl J, Linz J, Krügel T, Stensmyr MC, Hansson BS. 2010. Pollination strategies in Cretan arum lilies. *Biological Journal of the Linnean Society* **101**: 991–1001.

Urru I, Stensmyr MC, Hansson BS. 2011. Pollination by brood-site deception. *Phytochemistry* **72**: 1655–1666.

Wagner AM, Krab K, Wagner MJ, Moore AL. 2008. Regulation of thermogenesis in flowering Araceae: the role of the alternative oxidase. *Biochimica et Biophysica Acta* **1777**: 993–1000.

Walsh GC, Posse MC. 2003. Abundance and seasonal distribution of predatory coprophilous Argentine rove beetles (Coleoptera: Staphylinidae), and their effects on dung breeding flies. *Coleopterisits Bulletin* **57**: 43–50.

Watling JR, Robinson SA, Seymour RS. 2006. Contribution of the alternative pathway to respiration during thermogenesis in flowers of the sacred lotus. *Plant Physiology* **140**: 1367–1373.

Watling JR, Grant NM, Miller RE, Robinson SA. 2008. Mechanisms of thermoregulation in plants. *Plant Signaling & Behavior* **3**: 595–597.

Wiegmann BM, Trautwein MD, Winkler IS, *et al.* 2011. Episodic radiations in the fly tree of life. *Proceedings of the National Academy of Sciences, USA* **108**: 5690–5695.

Willson MF, Hennon PE. 1997. The natural history of western skunk cabbage (*Lysichiton americanum*) in southeast Alaska. *Canadian Journal of Botany* **75**: 1022–1025.